

# Developmental ROS individualizes organismal stress resistance and lifespan

<https://doi.org/10.1038/s41586-019-1814-y>

Received: 29 January 2019

Accepted: 18 October 2019

Published online: 4 December 2019

Daphne Bazopoulou<sup>1</sup>, Daniela Knoefler<sup>1</sup>, Yongxin Zheng<sup>2,3</sup>, Kathrin Ulrich<sup>1</sup>, Bryndon J. Oleson<sup>1</sup>, Lihan Xie<sup>1</sup>, Minwook Kim<sup>1</sup>, Anke Kaufmann<sup>1</sup>, Young-Tae Lee<sup>4</sup>, Yali Dou<sup>4</sup>, Yong Chen<sup>5</sup>, Shu Quan<sup>2,3</sup> & Ursula Jakob<sup>1\*</sup>

A central aspect of aging research concerns the question of when individuality in lifespan arises<sup>1</sup>. Here we show that a transient increase in reactive oxygen species (ROS), which occurs naturally during early development in a subpopulation of synchronized *Caenorhabditis elegans*, sets processes in motion that increase stress resistance, improve redox homeostasis and ultimately prolong lifespan in those animals. We find that these effects are linked to the global ROS-mediated decrease in developmental histone H3K4me3 levels. Studies in HeLa cells confirmed that global H3K4me3 levels are ROS-sensitive and that depletion of H3K4me3 levels increases stress resistance in mammalian cell cultures. In vitro studies identified SET1/MLL histone methyltransferases as redox sensitive units of the H3K4-trimethylating complex of proteins (COMPASS). Our findings implicate a link between early-life events, ROS-sensitive epigenetic marks, stress resistance and lifespan.

Genetic effects are estimated to account for only 10–25% of the observed differences in human lifespan<sup>1</sup>. However, the remaining differences are not entirely attributable to environmental factors. Even when isogenic animals, such as *Caenorhabditis elegans*, are cultivated under identical environmental conditions, individual lifespans can vary by more than 50-fold. These results suggest that other, more stochastic factors account for variations in lifespan. Previous studies in *C. elegans* revealed that as early as day 1 of adulthood, subpopulations of longer-lived animals emerge<sup>2</sup>. We therefore focused on the concept that specific fluctuating signals during development might differentially affect processes that determine lifespan. We investigated the idea that ROS<sup>3</sup> might serve as early lifespan-determining modulators in *C. elegans*. This idea was built on *C. elegans* studies, which showed (1) that significant lifespan extension occurs following exposure to pharmacologically generated ROS in young adults<sup>4</sup> or by altering mitochondrial activity during development<sup>5</sup>, (2) that exposure of nematodes to non-lethal concentrations of ROS leads to increased stress resistance and longevity, a phenomenon termed mitohormesis<sup>4,6</sup> and (3) that individual larvae of a synchronized wild-type population exhibit large variations in endogenous ROS levels<sup>7</sup>.

## Early-life ROS affect adult redox states

To investigate whether and how developmental ROS levels affect *C. elegans* later in life, we used wild-type N2 worms that ubiquitously express the integrated redox-sensing protein Grx1-roGFP2, which faithfully responds to the cellular ratio of oxidized and reduced glutathione (GSSG:GSH)<sup>8</sup>. Consistent with previous peroxide measurements<sup>7</sup>, L2 larvae revealed a significantly more oxidizing redox environment and substantially larger individual differences than young adults, which

exhibited a maximally reduced environment with smaller inter-individual differences (Extended Data Fig. 1a). With increasing age, the average redox state became more oxidizing and individual differences in redox status re-emerged. Subsequent analysis of about 16,000 age-synchronized L2 larvae using a reconfigured large particle BioSorter (Extended Data Fig. 1b) confirmed our microscopy studies and showed that the GSSG:GSH ratio varies widely among individuals (Fig. 1a). We sorted and binned L2 worms with redox states 2–3 standard deviations above (L2<sup>ox</sup>) or below (L2<sup>red</sup>) the mean population (L2<sup>mean</sup>) (Fig. 1a, Extended Data Fig. 1c), and confirmed their different redox states by fluorescence microscopy (Fig. 1b, Extended Data Fig. 2a–d). Notably, L2<sup>ox</sup> and L2<sup>red</sup> worms did not differ significantly in size, reproductive activity, mitochondrial respiratory chain function or glycolytic flux (Extended Data Fig. 3a–f), excluding the possibility that more extreme early-life redox states affect development or other relevant physiological parameters. Subsequent redox analysis of sorted L2<sup>ox</sup> and L2<sup>red</sup> worms showed that all animals become similarly reduced in young adulthood and become more oxidized as they age (Fig. 1c). By day 7 of adulthood, however, the L2<sup>ox</sup> worms were significantly more reduced than the L2<sup>red</sup> worms. The trigger of the transient increase in GSSG:GSH ratios during early development and the mechanisms that cause the observed switch in endogenous redox states during adulthood are unknown. However, our results demonstrate that a synchronized population of *C. elegans* larvae contains subpopulations with redox environments that imprint information that becomes relevant later in life.

## Early-life ROS extend lifespan

To investigate potential downstream effects of the observed variations in developmental redox levels, we compared stress resistance

<sup>1</sup>Department of Molecular, Cellular and Developmental Biology, University of Michigan, Ann Arbor, MI, USA. <sup>2</sup>State Key Laboratory of Bioreactor Engineering, East China University of Science and Technology, Shanghai, China. <sup>3</sup>Shanghai Collaborative Innovation Center for Biomanufacturing (SCICB), Shanghai, China. <sup>4</sup>Department of Pathology, Michigan Medicine, Ann Arbor, MI, USA. <sup>5</sup>State Key Laboratory of Molecular Biology, National Center for Protein Science Shanghai, CAS Center for Excellence in Molecular Cell Science, Shanghai Institute of Biochemistry and Cell Biology, Chinese Academy of Sciences, Shanghai, China. \*e-mail: [ujakob@umich.edu](mailto:ujakob@umich.edu)

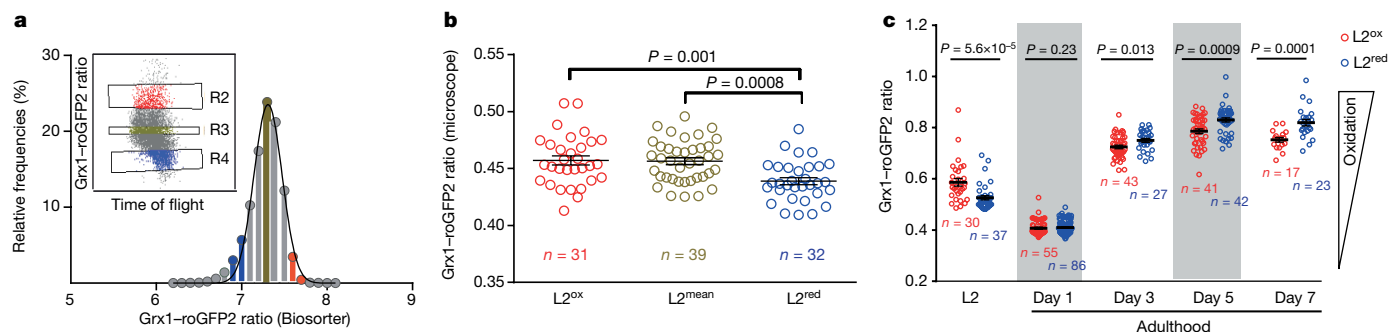


**Fig. 1 | Endogenous redox state in an age-synchronized population of *C.***

**elegans** larvae. **a**, Distribution of intracellular glutathione redox potential (Grx1-roGFP2 ratio) of an L2-staged *N2* *grx1-17::Grx1-roGFP2* population. L2 worms with Grx1-roGFP2 ratios between 2 and 3 standard deviations above ( $L2^{ox}$ ; red line and inset, R2) or below ( $L2^{red}$ ; blue line and inset, R4) the mean were sorted and compared with worms with mean Grx1-roGFP2 ratios ( $L2^{mean}$ ; green line and inset, R3).  $n = 15,599$  worms. **b**, Representative microscopy analysis of the Grx1-roGFP2 ratio of individual worms (dots) of the  $L2^{ox}$ ,  $L2^{mean}$

and  $L2^{red}$  subpopulations.  $n$ , number of worms; one-way ANOVA with Tukey correction. The experiment was repeated four more times with similar results (see Extended Data Fig. 2a–d). **c**, Longitudinal analysis of the redox state. Sorted  $L2^{ox}$  and  $L2^{red}$  worms were cultivated at 20 °C and the Grx1-roGFP2 ratio of worms in each subpopulation was determined microscopically at the indicated time points.  $n$ , number of worms; two-sided Mann–Whitney  $U$ -test. In **b**, **c**, bars represent mean and error bars show s.e.m.

and lifespan of the sorted worms. We found that compared with  $L2^{red}$  worms,  $L2^{ox}$  worms were significantly more resistant to heat shock (Extended Data Fig. 3g), about 30% longer lived after the initial heat-shock treatment (Fig. 2a) and substantially longer lived when grown in the presence of oxidants such as paraquat (Fig. 2b) or juglone (Extended Data Table 1). Moreover,  $L2^{ox}$  worms displayed an increase of up to 18% in median lifespan and a 1–4-day increase in maximal lifespan (Fig. 2c, Extended Data Fig. 2e–i, Extended Data Table 2). This clear correlation between increased GSSG:GSH ratios, stress resistance and lifespan suggested that a subpopulation of synchronized worms undergo naturally occurring hormesis during early development. Indeed, when we generated a more oxidizing environment in an entire population of worms by exposing them to 1 mM paraquat for 10 h during their L2 stage, the entire population became longer-lived (Fig. 2d with inset). Treatment of L2 worms with 10 mM *N*-acetylcysteine (NAC) for 10 h did not substantially alter the redox state of the population and had no significant lifespan effect. By conducting the same experiments with previously sorted subpopulations, however, we found that a 10-h NAC treatment decreased the lifespan of  $L2^{ox}$  worms but not of the already reduced  $L2^{red}$  worms, whereas a 10-h paraquat exposure increased the lifespan of  $L2^{red}$  worms but not of the already oxidized  $L2^{ox}$  worms (Fig. 2e, f, Extended Data Table 3). These results provide evidence that transient changes in the redox environment during early development are sufficient to positively affect the lifespan of *C. elegans*.

### Early-life ROS reduce H3K4me3 levels

To gain insights into the mechanisms by which a transient increase in the cellular redox state during development might cause an increase in stress resistance and lifespan, we first conducted quantitative PCR with reverse transcription (RT-PCR) to examine changes in mRNA levels of commonly assessed heat-shock- (Fig. 3a) and oxidative stress-related genes (Extended Data Fig. 4a). Unexpectedly,  $L2^{ox}$  and  $L2^{red}$  worms did not significantly differ in the steady-state expression levels of any of these genes. However, on exposure to heat-shock conditions,  $L2^{ox}$  worms showed a significantly increased capacity to upregulate heat-shock gene expression compared with  $L2^{red}$  worms (Fig. 3a). Changes in transcript levels of heat-shock factor HSF-1 were not significantly different, suggesting that the transcriptional stimulation in  $L2^{ox}$  worms is a result of either specific changes in HSF-1 activity, its subcellular localization or the accessibility of heat-shock promoter<sup>9</sup>.

Subsequent RNA-sequencing analysis from four independent large-scale sorting experiments identified 191 upregulated and 136

downregulated genes in  $L2^{ox}$  worms compared with  $L2^{red}$  worms (Extended Data Fig. 4b). We were unable to draw any clear link between the differentially expressed genes (DEGs) and previously identified sets of stress- or longevity-related genes (Extended Data Fig. 4c, Supplementary Table 1). However, 26 of the 191 upregulated genes overlapped with a set of 101 genes previously shown to be upregulated in worms lacking the absent small homeodisc protein ASH-2<sup>10</sup> (expected overlap if no correlation  $<1$ ;  $P = 1.7 \times 10^{-22}$ , hypergeometric probability) (Fig. 3b, Supplementary Table 1). ASH-2 is a component of the highly conserved histone methylation complex COMPASS, which, together with a member of the SET1/MLL histone methyltransferase family (SET-2 in *C. elegans*) and other partner proteins, causes trimethylation of lysine 4 in histone H3 (H3K4me3)<sup>11</sup>. H3K4me3 is primarily found at transcription start sites, where the modification is thought to mark and maintain transcriptionally active genes<sup>12</sup>. Recent studies in *C. elegans* revealed that H3K4me3 marks associated with transcription start sites are set during early development and remain stable throughout life<sup>13</sup>. Indeed, analysis of published chromatin immunoprecipitation data revealed that about 25% of DEGs that we identified in  $L2^{ox}$  worms associates with H3K4me3 marks that appear to be set during development (Extended Data Fig. 4d, e). Furthermore, we found a highly significant overlap between DEGs in  $L2^{ox}$  worms and DEGs in strains lacking the H3K4me3 readers SET-9 or SET-26<sup>14</sup>, similar to the overlap between *ash-2* knockdown and *set-9* or *set-26* deletion strains (Extended Data Fig. 4f, g). On the basis of these results, we decided to analyse the global H3K4me3 abundance in  $L2^{ox}$  and  $L2^{red}$  worms by western blotting using antibodies against H3K4me3. We tested the subpopulations of seven independent sorting experiments and found a clear and highly reproducible reduction of more than 25% in global H3K4me3 levels in  $L2^{ox}$  worms (Fig. 3c, Extended Data Fig. 5a). By contrast, other marks, such as H3K27ac or H3K27me3, were not significantly different between the two subpopulations (Extended Data Fig. 5b, c). These results strongly suggest a link between endogenous ROS levels, H3K4 trimethylation levels and gene regulation.

### A redox-sensitive histone mark

RNA-sequencing analysis of  $L2^{ox}$  and  $L2^{red}$  worms did not reveal any transcriptional changes in components of the COMPASS complex. This result suggested that the activity rather than the level of the H3K4me3 complex is affected by the redox environment. To directly test whether the H3K4me3 machinery is ROS-sensitive, we attempted to purify the *C. elegans* proteins for in vitro methylation assays. However,

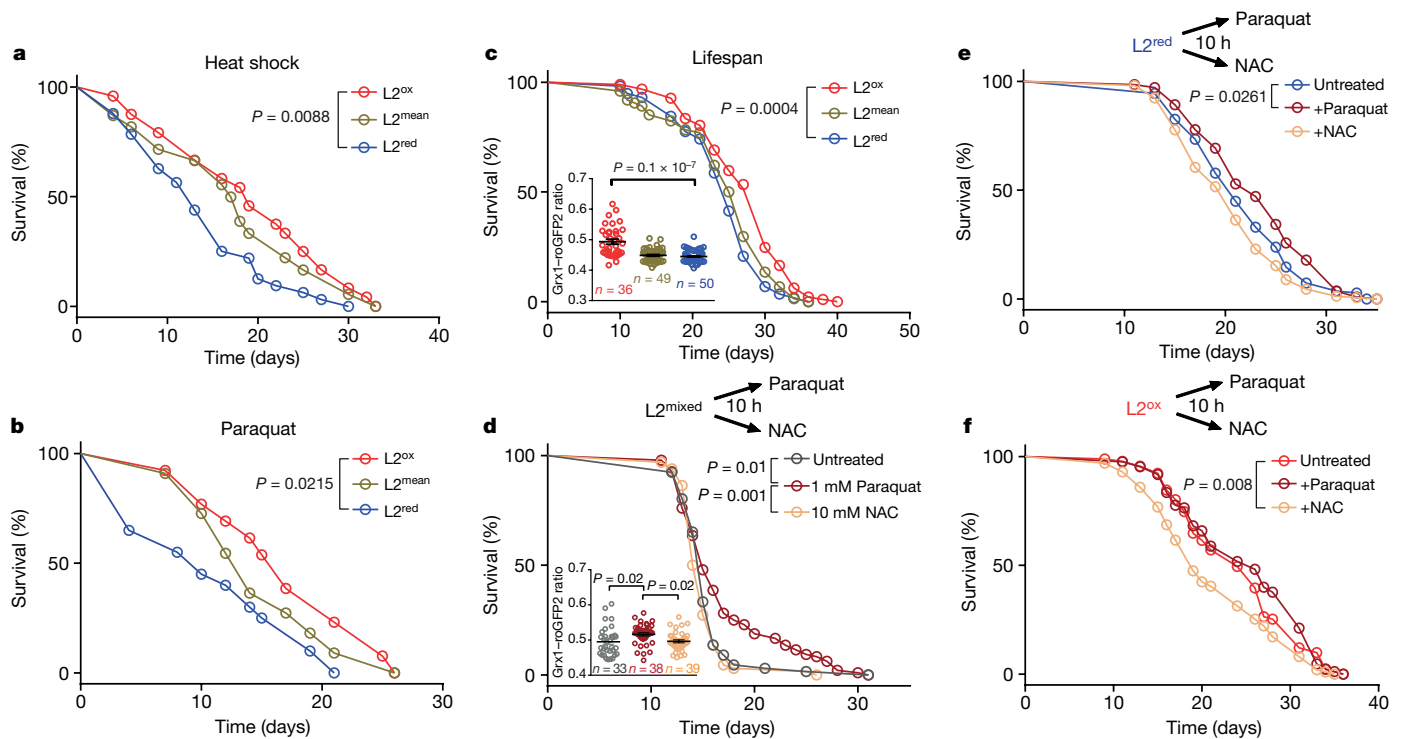


**Fig. 2 | Oxidized L2 subpopulations show increased stress resistance and longer lifespan.** Experiments were performed with  $N2jrls2[Prpl-17::Grx1-roGFP2]$  worms sorted into  $L2^{ox}$ ,  $L2^{mean}$  and  $L2^{red}$  subpopulations. **a**, Representative survival curves of sorted worms that survived heat-shock treatment. **b**, Representative survival curves of sorted worms cultivated on NGM plates supplemented with 2 mM paraquat. **c**, Representative survival curves of sorted worms. See Extended Data Fig. 2e–i for repetitions. Inset, Grx1-roGFP2 ratio of individual worms (dots) after sorting.  $n$ , number of worms; two-sided unpaired  $t$ -test. **d**, Representative survival curves of a non-

sorted (mixed) worm population either untreated or treated at the L2 stage with 1 mM paraquat or 10 mM NAC for 10 h. Inset, Grx1-roGFP2 ratio of individual worms (dots) after treatment.  $n$ , number of worms; one-way ANOVA with Tukey correction. Data in insets are mean  $\pm$  s.e.m. **e**, **f**, Representative survival curves of an  $L2^{red}$  (**e**) or  $L2^{ox}$  (**f**) subpopulation, either untreated or after a 10-h treatment with 1 mM paraquat or 10 mM NAC. The specific sorting events, number of individuals, repetitions and statistical analysis (log-rank) for each of the datasets shown in this figure are presented in Extended Data Tables 1–3.

this turned out to be impossible owing to their instability. By contrast, the mammalian members of the COMPASS have been previously used in H3K4 methylation assays *in vitro*<sup>15</sup>. To determine whether H3K4 trimethylation is a redox-sensitive process in mammalian cells, we subjected HeLa cells to non-lethal  $H_2O_2$  treatment and investigated global H3K4me3 levels. Consistent with our findings in *C. elegans*, we observed a global decrease of about 30% in H3K4me3 levels within 30 min of peroxide treatment (Fig. 3d, Extended Data Fig. 5d), without detectable changes in steady-state levels of two of the main COMPASS components (Extended Data Fig. 5e, f). We subsequently purified the mammalian core COMPASS proteins—that is, the SET domain of MLL1, which catalyses lysine-directed histone methylation<sup>16</sup>, ASH2L, WDR5 (human homologue of *C. elegans* WDR-5.1) and RBBP5. We then treated the individual proteins with peroxide for 30 min, removed the oxidant, recombined the proteins and tested them for *in vitro* histone methylation activity. Notably, among these proteins, only the SET-domain of MLL1 appeared to be reproducibly peroxide-sensitive (Fig. 3e, Extended Data Fig. 5g, h). Incubation of the peroxide-inactivated SET domain with thiol-reducing dithiothreitol (DTT) restored the original activity, strongly suggesting that thiol oxidation is responsible for the reversible inactivation (Fig. 3e, Extended Data Fig. 5g, h). Analysis of the SET domain of other SET1/MLL-family members<sup>17</sup>, including SET1A, the most closely related human homologue of *C. elegans* SET-2<sup>18</sup> (Extended Data Fig. 5i), SET1B (Extended Data Fig. 5j) and a version of MLL1 lacking the cysteine-containing GST-tag used for purification (Extended Data Fig. 5h) demonstrated that sensitivity towards peroxide is a universal feature for SET1/MLL family members. To investigate which of the seven cysteines in the SET domain of MLL1 might be sensitive to

reversible thiol oxidation, we conducted direct (Extended Data Fig. 5k, l) and reverse thiol trapping (Fig. 3f) on oxidized and reduced MLL1 SET domains using the 500-Da thiol-reactive compound 4-acetamido-4'-maleimidylstilbene-2,2'-disulfonic acid (AMS), followed by SDS-PAGE<sup>19</sup>. Analysis of the migration behaviour of thiol-trapped oxidized versus reduced MLL1 SET domain suggested that peroxide treatment leads to the formation of two intramolecular disulfide bonds. Subsequent mass spectrometry analysis of *in vitro*-modified cysteines confirmed these results and revealed that at least four of the five absolutely conserved cysteines in the SET domain are highly sensitive to oxidation (Extended Data Fig. 5m–o). To our knowledge, H3K4me3 is the only histone methylation mark and MLL1 is the only histone methyltransferase that is known to be posttranslationally redox-regulated.

### H3K4me3 modulates stress resistance

Our studies raised the possibility that redox-mediated inactivation of the lone SET1/MLL-homologue in the oxidized subpopulation of *C. elegans* (that is, SET-2) leads to a reduction in global H3K4me3 levels, which causes increased stress resistance and longevity. This theory was supported by recent studies showing that deleting or knocking down components of COMPASS in *C. elegans* increases lifespan<sup>10</sup>. Indeed, strains with either deleted (that is, *set-2* or *wdr-5.1*) or depleted (that is, *ash-2*) members of COMPASS were significantly more heat stress resistant than respective control strains or a strain deficient in the H3K4me3-demethylase RBR-2 (Fig. 3g). In addition, and comparable to results obtained with  $L2^{ox}$  worms, we found that worms deficient in H3K4me3 (Extended Data Fig. 6a–c) showed a substantially increased

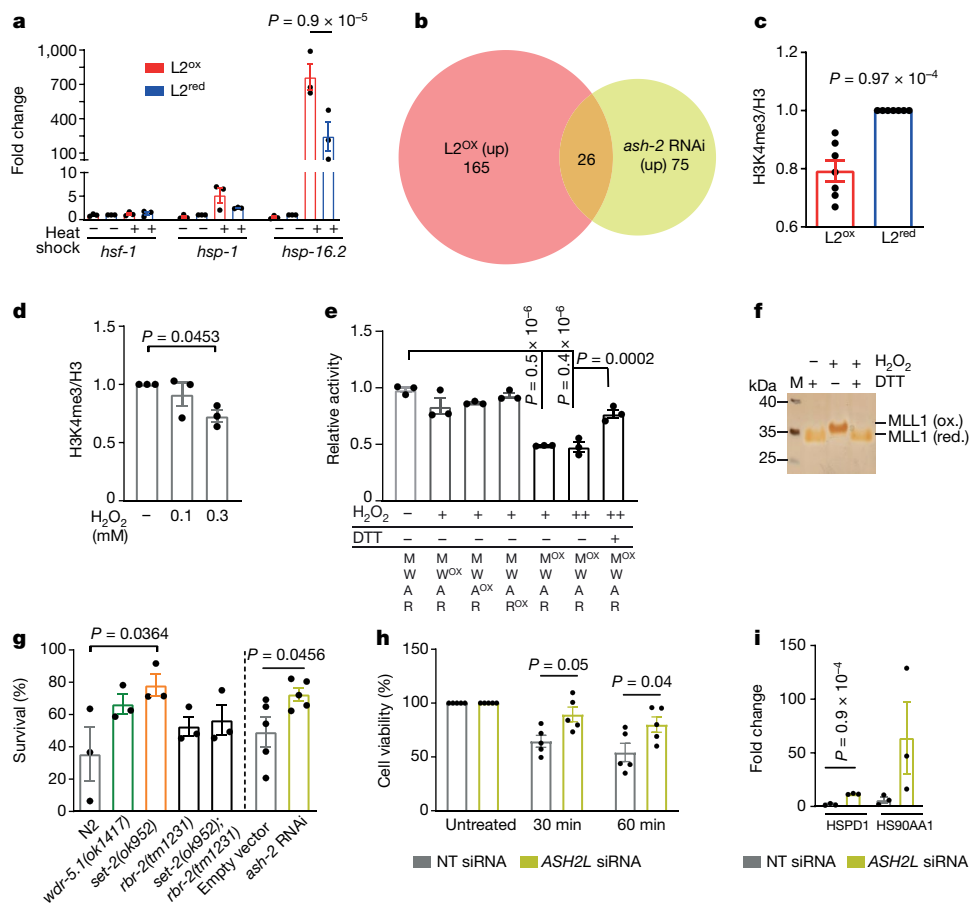


**Fig. 3 | H3K4me3 is a redox-sensitive histone modification involved in stress gene expression and resistance.** **a**, Transcripts of heat-shock-associated genes in sorted subpopulations before and after heat shock.  $n = 3$  independent sorting experiments; two-way ANOVA with Tukey correction. **b**, Venn diagram of upregulated genes in  $L2^{ox}$  and *ash-2* RNAi worms<sup>10</sup> (complete list in Supplementary Table 1). **c**, Quantification of global H3K4me3 levels in  $L2^{ox}$  and  $L2^{red}$  worms.  $n = 7$  independent sorting experiments; unpaired two-sided *t*-test. **d**, Quantification of H3K4me3 levels in HeLa cells before and after  $H_2O_2$  treatment.  $n = 3$  independent experiments; one-way ANOVA with Dunnett correction. **e**, In vitro histone methyltransferase assays with the purified core COMPASS proteins MLL1 (M), WDR5 (W), ASH2L (A) and RBBP5 (R); OX in superscript indicates that the protein is pre-treated with 1 mM (+) or 2 mM (++)  $H_2O_2$  for 30 min before the activity assay. DTT was added after the  $H_2O_2$  treatment as indicated.  $n = 3$  independent experiments; one-way ANOVA with

Sidak correction. **f**, Reverse thiol trapping of oxidized and reduced MLL1 SET domain. A 500-Da mass increase per oxidized thiol can be detected on non-reducing SDS-PAGE. M, protein marker. **g**, Heat-shock survival of wild-type, *wdr-5.1*, *set-2*, *rbr-2* and *set2/rbr-2* worms after 48 h ( $n = 3$  independent experiments; one-way ANOVA with Dunnett correction) or *N2/jrIs2[Prpl-17::Grx1-roGFP2]* worms treated with *ash-2* or control RNAi after 24 h ( $n = 5$  independent experiments; two-sided unpaired *t*-test). **h**, Heat-shock survival of HeLa cells treated with *ASH2L* siRNA.  $n = 5$  independent experiments; two-way ANOVA with Tukey correction. **i**, Transcript levels of heat-shock genes after 30-min heat stress treatment of HeLa cells treated with *ASH2L* siRNA. NT, non-targeting.  $n = 3$  independent experiments; two-sided unpaired *t*-test. Data in **a**, **c–e** and **g–i** are mean  $\pm$  s.e.m. For blot and gel source images, see Supplementary Figs. 1–3.

transcriptional response after heat shock (Extended Data Fig. 6d, e). We obtained very similar results with HeLa cells depleted of ASH2L by short interfering RNA (siRNA) treatment (Extended Data Fig. 6f), which were more resistant to heat stress (Fig. 3h) and demonstrated an augmented transcriptional response to heat stress compared with control siRNA-treated cells (Fig. 3i). These results strongly suggested that the downstream effects of H3Kme3 depletion on stress resistance and longevity are conserved.

Finally, to test whether downregulation of H3K4me3 levels is sufficient to increase heat-shock resistance and lifespan in  $L2^{ox}$  worms, we generated *ash-2* or *set-2* RNA interference (RNAi)-mediated knockdown worms expressing the Grx1-roGFP2 redox sensor protein and sorted the synchronized  $L2$  population as before. We detected no significant difference in the relative distribution or range of GSSG:GSH ratios between knockdown and control RNAi worms (Extended Data Fig. 6g). However, the sorted  $L2^{ox}$  and  $L2^{red}$  subpopulations of *ash-2* and *set-2* RNAi worms no longer exhibited any difference in heat-shock sensitivity (Fig. 4a, b) or lifespan (Fig. 4c, d, Extended Data Tables 2 and 4). Similarly, there was

no life-prolonging effect when we treated *ash-2* or *set-2* RNAi worms with paraquat for 10 h at the  $L2$  larval state (Extended Data Fig. 6h, Extended Data Table 4). These results imply that downregulation of H3K4me3 levels is both necessary and sufficient to increase heat-shock resistance and lifespan in the oxidized subpopulation of worms.

### Conclusions

In 2010, Cynthia Kenyon suggested that a stochastic event might flip an epigenetic switch or set in motion a chain of events that promotes ageing<sup>20</sup>. Our studies have revealed that variations in endogenous ROS during development—potentially caused by locally different growth conditions—contribute to the variation in lifespan observed in synchronized populations of *C. elegans*. Animals that accumulate high levels of ROS during development apparently undergo an endogenous hormesis event, which, as previously observed with exogenous ROS treatment<sup>21</sup>, increases stress resistance and lifespan. This might serve as a bet-hedging strategy to provide subpopulations of worms with

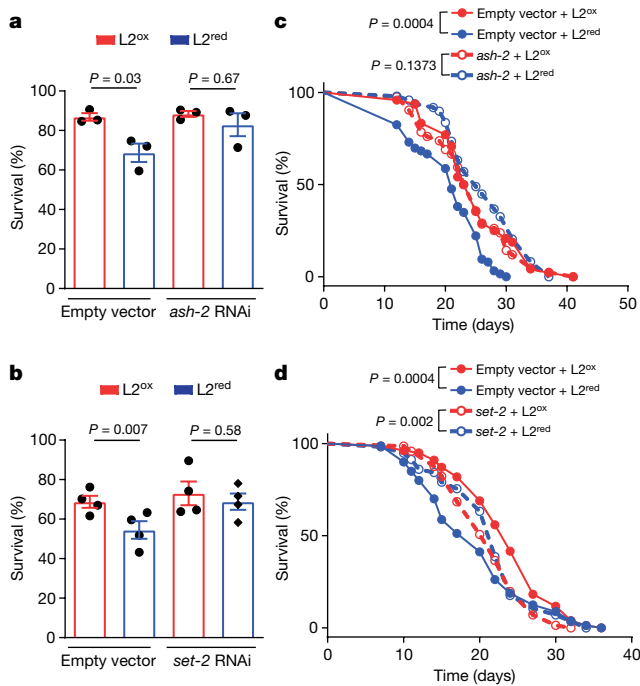


**Fig. 4 | An intrinsically oxidizing environment confers increased stress resistance via downregulation of global H3K4me3 levels. a, b,** Survival of *N2jrls2[Prpl-17::Grx1-roGFP2]* worms treated with *ash-2* (a) or *set-2* (b) RNAi, sorted into L2<sup>ox</sup> and L2<sup>red</sup> and counted 24 h after heat shock.  $n = 3$  (a) and  $n = 4$  (b) independent experiments; two-way ANOVA with Tukey correction. Data are mean  $\pm$  s.e.m. **c, d,** Representative survival curves of *N2jrls2[Prpl-17::Grx1-roGFP2]* worms treated with *ash-2* (c) or *set-2* (d) RNAi and sorted into L2<sup>ox</sup> and L2<sup>red</sup>. For  $n$  numbers, repetitions and statistics (log-rank) in c and d, see Extended Data Tables 2 and 4.

improved survival during stress. Our studies reveal the underlying mechanism of ROS-mediated hormesis by demonstrating that global H3K4me3 levels are redox-sensitive and decrease in response to oxidative stress. On the basis of the findings that decreased global H3K4me3 levels increase stress resistance and *C. elegans* lifespan<sup>10</sup>, we postulate that we have identified a stochastic event, the epigenetic switch and the chain of events that are set in motion during early development to increase lifespan.

Recent studies in *C. elegans* demonstrated that H3K4me3 marks within gene bodies are set during adulthood and change with age<sup>13</sup>. By contrast, H3K4me3 enrichment at transcription start sites—which is thought to provide a ‘memory’ of actively transcribed genes—is set during development and remains stable throughout the lifespan<sup>13</sup>. This result probably explains how transient redox-mediated changes in H3K4me3 levels during development are sufficient to exert long-lasting effects despite the marked changes in the redox environment during adulthood. Our finding that organisms with lower levels of H3K4me3 show an increased transcriptional response to stress conditions is initially counterintuitive, given that H3K4me3 is widely considered an activating mark<sup>12</sup>. However, our results are fully consistent with yeast studies, which have shown that reduction of H3K4me3 levels causes substantially more robust gene expression changes upon stress treatment<sup>22</sup>. The extent to which this increase in transcriptional capacity of stress-related genes is linked to the observed lifespan extension, however, remains to be determined. A substantial number of genes involved in lipid metabolism were found to be downregulated in L2<sup>ox</sup> worms (Extended Data Fig. 4c, Supplementary Table 1). This is notable, as increased lipid storage and altered lipid signalling have previously been linked to increased lifespans of a variety of different organisms<sup>23</sup>

and found to have a role in the extension of lifespan of worms globally deficient in H3K4me3 levels<sup>24</sup>. Further investigation is needed to reveal how the transient downregulation of H3K4me3 levels selectively during development can elicit similarly profound lifespan-altering effects. Our ability to change the lifespan of an entire population with a simple 10-h exposure to ROS during development suggests that we have identified a time window and a mechanism that helps to individualize lifespan in animals. This study provides a foundation for future work in mammals, in which very early and transient metabolic events in life seem to have equally profound impacts on lifespan<sup>25</sup>.

## Online content

Any methods, additional references, Nature Research reporting summaries, source data, extended data, supplementary information, acknowledgements, peer review information; details of author contributions and competing interests; and statements of data and code availability are available at <https://doi.org/10.1038/s41586-019-1814-y>.

1. Finch, C. E. & Tanzi, R. E. Genetics of aging. *Science* **278**, 407–411 (1997).
2. Rea, S. L., Wu, D., Cypser, J. R., Vaupel, J. W. & Johnson, T. E. A stress-sensitive reporter predicts longevity in isogenic populations of *Caenorhabditis elegans*. *Nat. Genet.* **37**, 894–898 (2005).
3. Holmström, K. M. & Finkel, T. Cellular mechanisms and physiological consequences of redox-dependent signalling. *Nat. Rev. Mol. Cell. Biol.* **15**, 411–421 (2014).
4. Schulz, T. J. et al. Glucose restriction extends *Caenorhabditis elegans* life span by inducing mitochondrial respiration and increasing oxidative stress. *Cell Metab.* **6**, 280–293 (2007).
5. Dillin, A. et al. Rates of behavior and aging specified by mitochondrial function during development. *Science* **298**, 2398–2401 (2002).
6. Ristow, M. & Schmeisser, S. Extending life span by increasing oxidative stress. *Free Radic. Biol. Med.* **51**, 327–336 (2011).
7. Knoefler, D. et al. Quantitative in vivo redox sensors uncover oxidative stress as an early event in life. *Mol. Cell* **47**, 767–776 (2012).
8. Gutschner, M. et al. Real-time imaging of the intracellular glutathione redox potential. *Nat. Methods* **5**, 553–559 (2008).
9. Labbadia, J. & Morimoto, R. I. Repression of the heat shock response is a programmed event at the onset of reproduction. *Mol. Cell* **59**, 639–650 (2015).
10. Greer, E. L. et al. Members of the H3K4 trimethylation complex regulate lifespan in a germline-dependent manner in *C. elegans*. *Nature* **466**, 383–387 (2010).
11. Shilatifard, A. The COMPASS family of histone H3K4 methylases: mechanisms of regulation in development and disease pathogenesis. *Annu. Rev. Biochem.* **81**, 65–95 (2012).
12. Guenther, M. G., Levine, S. S., Boyer, L. A., Jaenisch, R. & Young, R. A. A chromatin landmark and transcription initiation at most promoters in human cells. *Cell* **130**, 77–88 (2007).
13. Pu, M. et al. Unique patterns of trimethylation of histone H3 lysine 4 are prone to changes during aging in *Caenorhabditis elegans* somatic cells. *PLoS Genet.* **14**, e1007466 (2018).
14. Wang, W. et al. SET-9 and SET-26 are H3K4me3 readers and play critical roles in germline development and longevity. *eLife* **7**, e34970 (2018).
15. Dou, Y. et al. Regulation of MLL1 H3K4 methyltransferase activity by its core components. *Nat. Struct. Mol. Biol.* **13**, 713–719 (2006).
16. Southall, S. M., Wong, P. S., Odho, Z., Roe, S. M. & Wilson, J. R. Structural basis for the requirement of additional factors for MLL1 SET domain activity and recognition of epigenetic marks. *Mol. Cell* **33**, 181–191 (2009).
17. Shilatifard, A. Molecular implementation and physiological roles for histone H3 lysine 4 (H3K4) methylation. *Curr. Opin. Cell Biol.* **20**, 341–348 (2008).
18. Li, T. & Kelly, W. G. A role for Set1/MLL-related components in epigenetic regulation of the *Caenorhabditis elegans* germ line. *PLoS Genet.* **7**, e1001349 (2011).
19. Leichert, L. I. et al. Quantifying changes in the thiol redox proteome upon oxidative stress in vivo. *Proc. Natl Acad. Sci. USA* **105**, 8197–8202 (2008).
20. Kenyon, C. J. The genetics of ageing. *Nature* **464**, 504–512 (2010).
21. Yang, W. & Hekimi, S. A mitochondrial superoxide signal triggers increased longevity in *Caenorhabditis elegans*. *PLoS Biol.* **8**, e1000556 (2010).
22. Weiner, A. et al. Systematic dissection of roles for chromatin regulators in a yeast stress response. *PLoS Biol.* **10**, e1001369 (2012).
23. Hansen, M., Flatt, T. & Aguilaniu, H. Reproduction, fat metabolism, and life span: what is the connection? *Cell Metab.* **17**, 10–19 (2013).
24. Han, S. et al. Mono-unsaturated fatty acids link H3K4me3 modifiers to *C. elegans* lifespan. *Nature* **544**, 185–190 (2017).
25. Sun, L., Sadighi Akha, A. A., Miller, R. A. & Harper, J. M. Life-span extension in mice by preweaning food restriction and by methionine restriction in middle age. *J. Gerontol. A* **64A**, 711–722 (2009).

**Publisher's note** Springer Nature remains neutral with regard to jurisdictional claims in published maps and institutional affiliations.

© The Author(s), under exclusive licence to Springer Nature Limited 2019

# Article

## Methods

No statistical methods were used to predetermine sample size. The experiments were not randomized. The investigators were not blinded to allocation during experiments, unless otherwise noted, and outcome assessment.

### *C. elegans* strains, maintenance and lifespan assays

The following *C. elegans* strains were used in this study: PB020: *N2jrls2[Prpl-17::Grx-1-roGFP2]*, N2: Wild-type Bristol isolate, RB1304: *wdr-5.1(ok1417)*, RB1025: *set-2(ok952)*, ZR1: *rbr-2(tm1231)* and ABR9: *set-2(ok952);rbr-2(tm1231)*. Unless stated otherwise, worms were cultured at 20 °C. Standard procedures were followed for *C. elegans* strain maintenance<sup>26</sup>. Synchronization was performed using alkaline hypochlorite solution; eggs were allowed to hatch by overnight incubation in M9 medium during gentle shaking. Newly hatched, arrested L1 larvae were transferred onto standard nematode growth medium (NGM) plates seeded with live *E. coli* OP50. Lifespan studies were performed at 20 °C in the presence of fluorodeoxyuridine. Survival was scored every 2 days, and worms were censored if they crawled off the plate, hatched inside or lost vulva integrity during reproduction. The first day of adulthood was set as  $t = 0$ . Lifespan of unsorted worm populations were performed in a lifespan machine according to<sup>27</sup>. Survival plots were generated using GraphPad Prism. Lifespan data were analysed for statistical significance with log-rank (Mantel–Cox) or Gehan–Breslow–Wilcoxon test.

### Reconfiguration of BioSorter for ratiometric sorting

Lasers of wavelength 405 and 488 nm were used to excite the Grx1-roGFP2 sensor protein. Since the protein possesses a single emission maximum (~520 nm), the two lasers in the BioSorter (Union Biometrica) were realigned to sequentially illuminate single L2-staged worms as they passed through the flow cell, without emitting overlapping signals. This enabled collection of signals from 405- and 488-nm lasers separately, from two photon multipliers tubes. As a result, data were displayed as two groups of peaks (Extended Data Fig. 1b). Using the partial profiling feature (pp) of the FlowPilot-Pro software, we mapped the peaks corresponding to each laser that trace the fluorescent intensity and extinction signals. The extinction signal from the 488-nm laser was used to initially gate worms at the L2 stage larva (R1 gate, see Extended Data Fig. 1c). Oxidized, mean and reduced L2 worms were sorted from R2, R3 and R4 gates respectively, based on the peak 405 and 488-nm fluorescent intensities (inset in Fig. 1a).

### Microscopy

Worms were mounted on objective slides using 4 µl thermoreversible CyGEL (BioStatus; Fisher Scientific) and 2 µl of 50 mM levamisole for immobilization. Fluorescence and DIC images were acquired with an upright microscope equipped with a Photometrics Coolsnap HQ2 cooled CCD camera, a UPlan S-Apo 20× objective (NA 0.75) and a X-CITE exacte light source equipped with a closed feedback loop. For Grx1-roGFP2 fluorescence, an external filter wheel was used with excitation filters 420/40×, 500/20×, dual bandpass dichroic T515LPXR and a single emission filter 535/30×. Image analysis was performed in Metamorph (Molecular Devices) using a custom script. In brief, an intensity threshold was chosen by the user. Pixels above this threshold constitute regions of interest. Regions with very high signal in any channel (for example, fluorescent particles) were identified by applying an over-saturation threshold and excluded from regions of interest. Mean ratiometric values (excitation 420 nm–emission 535 nm/excitation 500 nm–emission 535 nm) of regions of interest were calculated after subtraction of background. Acquisition parameters were kept identical across all samples. For body-length measurements, worms were measured from the nose to the tail tip and analysis was performed with ImageJ.

### Brood size

L4-staged worms were transferred onto NGM plates and incubated at 15 °C. The parental animals were transferred daily to individual NGM

plates until the end of the reproductive period. The progeny of each animal was counted at the L2 or L3 stage.

### Cellular respiration

Real-time oxygen consumption rates and extracellular acidification rate were measured with a Seahorse XF<sup>96</sup> Analyzer (Seahorse Bioscience) as described<sup>28</sup>. In brief, 100 L2-staged worms were sorted directly into individual wells of 96-well Seahorse utility plates at a final volume of 200 µl of 10% M9. Acute effects of pharmacological inhibitors carbonyl cyanide-4(*p*-trifluor-methoxy)phenylhydrazone (FCCP), an accelerator of the electron transport chain (ETC) and sodium azide (NaN<sub>3</sub>), a complex IV and V inhibitor, were evaluated by injecting them during the run at final concentrations of 20 µM and 40 mM respectively.

### Heat-shock treatment

Heat shock was performed on solid OP50-seeded NGM plates wrapped in parafilm and submerged in a pre-heated water bath. For thermotolerance assays, worms were heat-shocked for 45 min at 38 °C. Survival was scored after 24 h and then until the death of the last worm by absence of touch response or pharyngeal pumping. For transcriptional response assays, worms were heat-shocked for 30 min at 35 °C. After 1 h recovery at 20 °C, worms were collected and snap-frozen in liquid nitrogen. All heat-shock treatments were applied to worms at the L2 stage.

### Treatments with NAC and paraquat

For survival assays, worms were cultivated on solid OP50-seeded NGM plates, supplemented with the indicated concentrations of NAC or paraquat. Survival was determined by absence of touch response or pharyngeal pumping. For transient exposure to compounds, worms were transferred into M9-media supplemented with OP50 and the indicated concentrations of NAC or paraquat for 10 h. Worms were harvested, washed three times with M9 and transferred onto regular OP50-seeded NGM plates.

### RNA extraction and real-time quantitative PCR

Worms at the L2 stage (3,000–5,000; whole population or after sorting) were grounded in Trizol reagent (Life Technologies) with sea sand and a pestle. After filtering of the sand, samples were vigorously shaken with chloroform, allowed to stand for 3 min at room temperature, and then centrifuged at 16,000g at 4 °C. The aqueous phase was then collected and RNA was purified using QIAGEN RNeasy RNA extraction columns according to the manufacturers' recommendations. HeLa cells were directly lysed in the culture dish by adding Trizol, as per manufacturers' recommendations. For RNA isolation, after addition of ethanol, the lysate was loaded onto QIAGEN RNeasy RNA extraction columns. cDNA synthesis was performed using PrimeScript 1st strand cDNA Synthesis Kit (Takara) and real-time quantitative PCR was performed using Radiant Green Lo-ROX qPCR Kit (Alkali Scientific), as per manufacturers' recommendations, in an Eppendorf Mastercycler epgradient S realplex<sup>2</sup> detection system. Relative expression was calculated from Cycle threshold values using the 2<sup>-ΔΔC<sub>t</sub></sup> method and the expression of genes of interest were normalized to housekeeping genes (*cdc-42*, *pmp-3*, *panactin*) and/or spiked-in luciferase (10 pg ml<sup>-1</sup> Trizol).

Primers used were *cdc-2*: 5'-AGCCATTCTGGCCGCTCTCG-3' and 5'-GCAACCGCTTCTCGTTGGC-3'; *pmp-3*: 5'-TTTGTGTCAATTGGTCATCG-3' and 5'-CTGTGTCAATGTCGTGAAGG-3'; *panactin*: 5'-TCGGTATGGACAGAAGGAC-3' and 5'-CATCCAGTTGGTGACGATA-3'; *sod-1*: 5'-AAAATGTGGAACCGTGCTG-3' and 5'-TGAACGTGGAATCCATGAA-3'; *sod-2*: 5'-GATTTGGAGCCTGTAATCAGTC-3' and 5'-GAAGAGCGATAGCTTCTTTGAC-3'; *sod-3*: 5'-CACTATTAAGCGCGACTTCGG-3' and 5'-CAATATCCCAACCATCCCCAG-3'; *ctl-2*: 5'-ATCCCAACATGATCTTTGA-3' and 5'-TGAGATTCTTCACTGGTTG-3'; *prdx-2*: 5'-CGACTCTGTCTTCTCTCAC-3' and 5'-GAAGATCATTGATGGTGAT-3'; *aak-2*: 5'-AAGTCTGGAGTTGGGAATACG-3' and 5'-GTATGCACTTCTTTGTGG AACC-3'; *hsf-1*: 5'-TCCGTATAAGAATGCCGACTAGG-3' and 5'-TAGCTTCTG

ATGTGGTTGAAGG-3'; *hsp-1*: 5'-GGACGTCTTCCAAGGATGA-3' and 5'-TCAAGATCTCGTCTGACTTG-3'; *hsp-16.2*: 5'-CTGTGAGACGTTGAGATTGATG-3' and 5'-CTTTACCACTATTTCCGTCAG-3'; *ash-2*: 5'-CGATCGAACACGGAACGA-3' and 5'-TGCCGGAATCTGCAGTTTTT-3', *set-2*: 5'-TCGAAGATTGAAGGTGAAGAGAG-3' and 5'-ATCATCTGTTTTGCGGAACTGTA-3'; HSPDI: 5'-TGCTGAGTTTTGAAATGACAA-3' and 5'-CAATCTGCTCTCAAATGGACA-3'; Hsp90AA1: 5'-GAAATCTGTAGAACC CAAATTTCAA-3' and 5'-TCTTTGGATACCTAATGCGACA-3'; luciferase: 5'-ACGTCTCCCGACGATGA-3' and 5'-GTCTTCCGTGCTCCAAAAC-3'.

### RNA-sequencing analysis

Total RNA from four biological replicates of worms sorted at the L2 stage (extracted as described above) was assessed for quality using the TapeStation (Agilent). Samples were prepared using the Illumina TruSeq Stranded Total RNA Library Prep kit (Illumina). Total RNA (100 ng) was rRNA-depleted using Ribo-Gone (Takara Bio). The rRNA-depleted RNA was then fragmented and copied into first strand cDNA using reverse transcriptase and random primers. The products were purified and enriched by PCR (15 cycles) to create the final cDNA library. The 3' prime ends of the cDNA were adenylated and ligated to adapters, including a 6-nt barcode unique for each sample. Final libraries were checked for quality and quantity by TapeStation and qPCR using Kapa's library quantification kit for Illumina Sequencing platforms (Kapa Biosystems). The samples were pooled, clustered on an Illumina cBot and sequenced on one lane of an Illumina HiSeq4000 flow cell, as paired-end 50-nt reads. The quality of the raw reads data for each sample (for example, low-quality scores, over-represented sequences, inappropriate GC content) was checked using FastQC (v.0.11.3). The Tuxedo Suite software package was used for the computational analysis of the RNA sequencing<sup>29,30</sup>. In brief, reads were aligned to the reference genome WS220 using TopHat (v.2.0.13) and Bowtie2 (v.2.2.1). Cufflinks/CuffDiff (v.2.1.1) was used for expression quantitation, normalization, and differential expression analysis, using reference genome WS220. For this analysis, we used parameter settings: "–multi-read-correct" to adjust expression calculations for reads that map in more than one locus, as well as "–compatible-hits-norm" and "–upper-quartile-norm" for normalization of expression values. Diagnostic plots were generated using the CummeRbund R package. Genes and transcripts were identified as being differentially expressed based on three criteria: test status = "OK", FDR ≤ 0.05, and fold change ≥ ±1.5. The Bioconductor Package GSEA was used to perform enrichment test analysis. The algorithm was modified from the original gene set enrichment analysis (GSEA)<sup>31</sup>, for better power. Gene sets were downloaded from sources indicated in Supplementary Table 1. All FDR corrected *P* values in this result are extremely significant (FDR ≈ 0).

### Western blot

Standard methods for western blotting were used for the detection of proteins from worm lysates. In brief, 3,000–5,000 L2-staged worms were collected in 20 µl of M9 buffer and snap frozen in liquid nitrogen. Laemmli loading buffer was added to the worm pellet (1:1 volume) and the samples were boiled for 5 min, separated by SDS–PAGE and transferred to PVDF membranes. Blots were blocked for 1 h with 5% milk in PBS and probed with anti-H3 (Abcam, ab1791; 1:2,000), anti-H3K4me3 (Abcam, ab8580; 1:1,000), anti-H3K27ac (Abcam, ab4729; 1:1,000), anti-H3K27me3 (Millipore, 07-449; 1:1,000), anti-ASH-2 (Abmart, X3-GSEFZ3, 1:1,000;) or anti-β-tubulin (Santa Cruz, sc-5274; 1:2,000) primary antibodies overnight at 4 °C. For the extraction of mammalian proteins, HeLa cells were treated with trypsin (Invitrogen, 25200056) washed twice with PBS and collected in lysis buffer (RIPA buffer, 1 mM PMSF, protease inhibitor cocktail and 1 mM EDTA; 0.5 ml lysis buffer per 5 × 10<sup>6</sup> cells). Samples were incubated for 45 min at 4 °C with constant agitation. Lysates were spun down (4 °C, 20 min, 12,000 rpm) and snap frozen in liquid nitrogen. Laemmli loading buffer was added to the lysates (1:1 volume) and the samples were boiled for

5 min, separated by SDS–PAGE and transferred to PVDF membranes. Blots were blocked for 1 h with 5% milk in PBS and probed with anti-H3 (Abcam, ab1791; 1:2,000), anti-H3K4me3 (Abcam, ab8580; 1:1,000), anti-ASH2L (Bethyl laboratories, polyclonal, A300-489A; 1:1,000), anti-MLL1 (Bethyl laboratories, polyclonal, A300-374A; 1:500) or anti-β-tubulin (Santa Cruz, sc-5274; 1:2,500) primary antibodies overnight at 4 °C. HRP conjugated anti-rabbit (ThermoScientific, 31460) and anti-mouse (ThermoScientific, 31430) secondary antibodies were used at 1:5,000 dilution for 1 h at room temperature. Proteins were detected using Clarity ECL western blotting substrate (BioRad) and signal was captured using a BioRad ChemiDoc Touch imaging system.

### *C. elegans* RNAi

*Escherichia coli* HT115 (DE3) strains transformed with vectors expressing dsRNA of the genes of interest (*ash-2*, *set-2*, *wdr-5.1*, empty pL4440) were obtained from the Ahlinger library (a gift from G. Sankovszki), sequence-verified and grown at 37 °C as per manufacturer's recommendations. L1 worms obtained from synchronized populations were placed onto NGM plates containing ampicillin (100 mg ml<sup>-1</sup>) and IPTG (0.4 mM) seeded with the respective bacteria. Worms were cultivated on either RNAi or the empty vector control bacteria for two generations.

### Mammalian cell culture and H<sub>2</sub>O<sub>2</sub> treatment

HeLa (EM-2-11ht) cells (a gift from J. Nandakumar and authenticated by STR) were cultured in DMEM (Life Technologies, 11995-065), supplemented with 10% Fetal Bovine Serum (Sigma-Aldrich, F4135) and 1% penicillin–streptomycin (Gibco, 15140-122) at 5% CO<sub>2</sub>. At 80% confluency, cells were washed with PBS (Life Technologies, 10010023) and treated with HBSS (Life Technologies, 14025-092) supplemented with 0.1 mM or 0.3 mM H<sub>2</sub>O<sub>2</sub> and incubated at 37 °C for 30 min.

### Mammalian siRNA and heat-shock treatment

Eight thousand cells were transfected with 4.8 pmol of *ASH2L* siRNA (Dharmacon, M-019831-01-0005) or non-targeting siRNA (Dharmacon, D-001210-02-05) using Lipofectamine RNAiMax (Invitrogen, 13778-150) in OPTI-MEM I Reduced serum medium (Gibco, 31985-062). For heat-shock treatment, cells were washed with PBS 72 h after siRNA transfection and placed in HBSS. Plates were wrapped with parafilm and submerged in a pre-heated water bath at 43 °C for the indicated time points. Viability was determined using the CellTiter-Glo Kit (Promega) as per manufacturer's recommendations. Luminescence was monitored on a FLUOstar Omega microplate reader (BMG Labtech).

### Histone methyltransferase activity assays

SET domains of SET1/MLL family proteins (MLL1, SET1A, SET1B), RBBP5 (full length), ASH2L (full length), and WDR5 (full length) were purified as previously described<sup>32</sup>. The purified proteins were diluted to 10 µM and incubated with 1 mM or 2 mM H<sub>2</sub>O<sub>2</sub> at 4 °C for one hour in the buffer 25 mM Tris-HCl, pH 8.0. For DTT recovery, 4 mM DTT was added after H<sub>2</sub>O<sub>2</sub> treatment and was incubated at 4 °C for 60 min. After oxidation, excess H<sub>2</sub>O<sub>2</sub> was removed by ultrafiltration. Methyltransferase assays were performed using H3 peptides (residues 1–20) with one additional Tyr-residue at the C terminus for accurate quantification of peptides. An enzyme-coupled continuous spectrophotometric assay system was employed to monitor the time course of the reaction<sup>33,34</sup>. This assay system, which monitors the appearance of the cofactor product (SAH) at an absorbance of 515 nm (that is, OD<sub>515</sub>) contained the following components: 25 mM Tris (pH 8.0), 320 nM AdoHcy nucleosidase, 480 nM adenine deaminase, 40 U l<sup>-1</sup> xanthine oxidase, 20,000 U l<sup>-1</sup> horseradish peroxidase, 4.5 mM 3,5-dichloro-2-hydroxybenzenesulfonic acid, 0.894 mM 4-aminophenazone, 40 µM MnCl<sub>2</sub>, 2.25 µM K<sub>4</sub>Fe(CN)<sub>6</sub>·3H<sub>2</sub>O, 200 µM S-adenosyl-methionine and 1 µM of the four mammalian proteins that constitute the minimal H3K4-methylating complex. All components were mixed in 30 µl volume in 384-well plate at room temperature, and the reaction was initiated by adding 400 µM

# Article

H3 peptide substrate. The OD<sub>515</sub> was monitored using a Synergy Neo Multi-Mode Reader (Bio-Tek) for 1 h at 28 °C. The slope of OD<sub>515</sub> versus time from the first 20 min linear range was converted into reaction rates. The relative activity for each complex without any H<sub>2</sub>O<sub>2</sub> pretreatment was set to 1. A buffer control was used to determine the baseline.

## In vitro protein oxidation and thiol trapping

Purified MLL1 SET domain (15 μM) was treated with either 2 mM DTT or 2 mM H<sub>2</sub>O<sub>2</sub> for 30 min at 4 °C or 30 °C. To stop the reaction, the H<sub>2</sub>O<sub>2</sub>-treated samples were mixed with catalase (0.5 mg ml<sup>-1</sup>). To reduce reversible thiol modifications the oxidized sample were treated with 4 mM DTT for 30 min at 30 °C. The reduced cysteines were blocked with 20 mM NEM (*N*-ethylmaleimide) before SDS-PAGE analysis. For reverse thiol trapping experiments, the samples were resuspended in a denaturing thiol-trapping buffer (2.3 M urea, 0.2% SDS, 10 mM EDTA, 200 mM Tris-HCl, pH 8.5) supplemented with 20 mM NEM for 30 min at 25 °C. Proteins were precipitated with 10% trichloroacetic acid (TCA). After centrifugation, the pellets were washed with 10% TCA and 5% TCA and re-dissolved in the denaturing thiol-trapping buffer supplemented with 4 mM DTT to reduce reversible thiol modifications. After 45 min of incubation at 30 °C, all new cysteine thiols were labelled with 25 mM AMS for 5 min at 25 °C. Proteins were analysed on SDS-PAGE under non-reducing conditions and visualized using silver staining. For the mass spectrometry analysis of the cysteine-containing peptides, iodoacetamide (IAM) was used instead of AMS to label reversibly oxidized cysteines. After SDS-PAGE under non-reducing conditions and Coomassie staining, protein bands were cut out, trypsin-digested, and analysed by nano liquid chromatography with tandem mass spectrometry (LC-MS/MS; MS Bioworks).

## Statistical analysis

The Prism software package (GraphPad Software 7) and the Microsoft Office 2010 Excel software package (Microsoft Corporation) were used to carry out statistical analyses. Information about statistical tests, *P* values and *n* numbers are provided in the respective figures and figure legends.

## Reporting summary

Further information on research design is available in the Nature Research Reporting Summary linked to this paper.

## Data availability

All relevant data are available and/or included with the manuscript as Source Data or Supplementary Information. RNA-sequencing data

have been uploaded to the Gene Expression Omnibus (GEO) database with accession number GSE138502.

- Brenner, S. The genetics of *Caenorhabditis elegans*. *Genetics* **77**, 71–94 (1974).
- Stroustrup, N. et al. The *Caenorhabditis elegans* Lifespan Machine. *Nat. Methods* **10**, 665–670 (2013).
- Koopman, M. et al. A screening-based platform for the assessment of cellular respiration in *Caenorhabditis elegans*. *Nat. Protocols* **11**, 1798–1816 (2016).
- Langmead, B., Trapnell, C., Pop, M. & Salzberg, S. L. Ultrafast and memory-efficient alignment of short DNA sequences to the human genome. *Genome Biol.* **10**, R25 (2009).
- Trapnell, C., Pachter, L. & Salzberg, S. L. TopHat: discovering splice junctions with RNA-Seq. *Bioinformatics* **25**, 1105–1111 (2009).
- Subramanian, A. et al. Gene set enrichment analysis: a knowledge-based approach for interpreting genome-wide expression profiles. *Proc. Natl Acad. Sci. USA* **102**, 15545–15550 (2005).
- Ng, S. B. et al. Exome sequencing identifies MLL2 mutations as a cause of Kabuki syndrome. *Nat. Genet.* **42**, 790–793 (2010).
- Dorgan, K. M. et al. An enzyme-coupled continuous spectrophotometric assay for S-adenosylmethionine-dependent methyltransferases. *Anal. Biochem.* **350**, 249–255 (2006).
- Southall, S. M., Cronin, N. B. & Wilson, J. R. A novel route to product specificity in the Suv4-20 family of histone H4K20 methyltransferases. *Nucleic Acids Res.* **42**, 661–671 (2014).

**Acknowledgements** We thank M. Malinouski and T. Mullins for assistance with the reconfiguration of the Biosorter; G. Csankovszki for antibodies, *C. elegans* RNAi feeding clones and comments; B. Braeckman for the N2/jrls2[Prpl-17::Grx-1-roGFP2] strain; J. Nandakumar for HeLa (EM-2-11ht) cells; the *Caenorhabditis* Genetics Center (funded by National Institutes of Health Infrastructure Program P40 OD010440) for *C. elegans* strains; the DNA Sequencing Core (BRCF), R. Tagett, W. Wu and the Bioinformatics Core of University of Michigan for RNA sequencing and data analysis; K. Wan for protein purification; R. Sawarkar and J. Labbadia for important suggestions; Jakob laboratory members for comments on the manuscript and J. Bardwell for critically reading the manuscript. Mass spectrometry was performed by MS Bioworks. This work was supported by NIH grants GM122506 and AG046799 as well as the Priority Program SPP 1710 of the Deutsche Forschungsgemeinschaft (Schw823/3-2) to U.J., a NIH T32 Career Training in the Biology of Aging grant to D.B., a NIH T32 Career Training in the Biology of Aging grant and a Bright Focus ADR Fellowship (A2019250F) to B.J.O., and the National Natural Science Foundation of China (31470737) to Y.C.

**Author contributions** D.B. conceived and conducted most experiments, performed data analysis and wrote the manuscript; D.K. conceived experiments and initiated work with the BioSorter; Y.Z. performed the in vitro methyltransferase assays; K.U. performed the reverse thiol trapping and prepared samples for mass spectrometry analysis; B.J.O. assisted with RNAi experiments and western blots for methylation marks in *C. elegans*; L.X. performed siRNA in HeLa cells; M.K. built and operated the lifespan instrument; A.K. assisted with worm sorting and produced brood size data; Y.-T.L. purified mammalian proteins; Y.D. conceived experiments and provided material; S.Q. and Y.C. conceived experiments; U.J. conceived experiments, conducted data analysis and wrote the manuscript.

**Competing interests** The authors declare no competing interests.

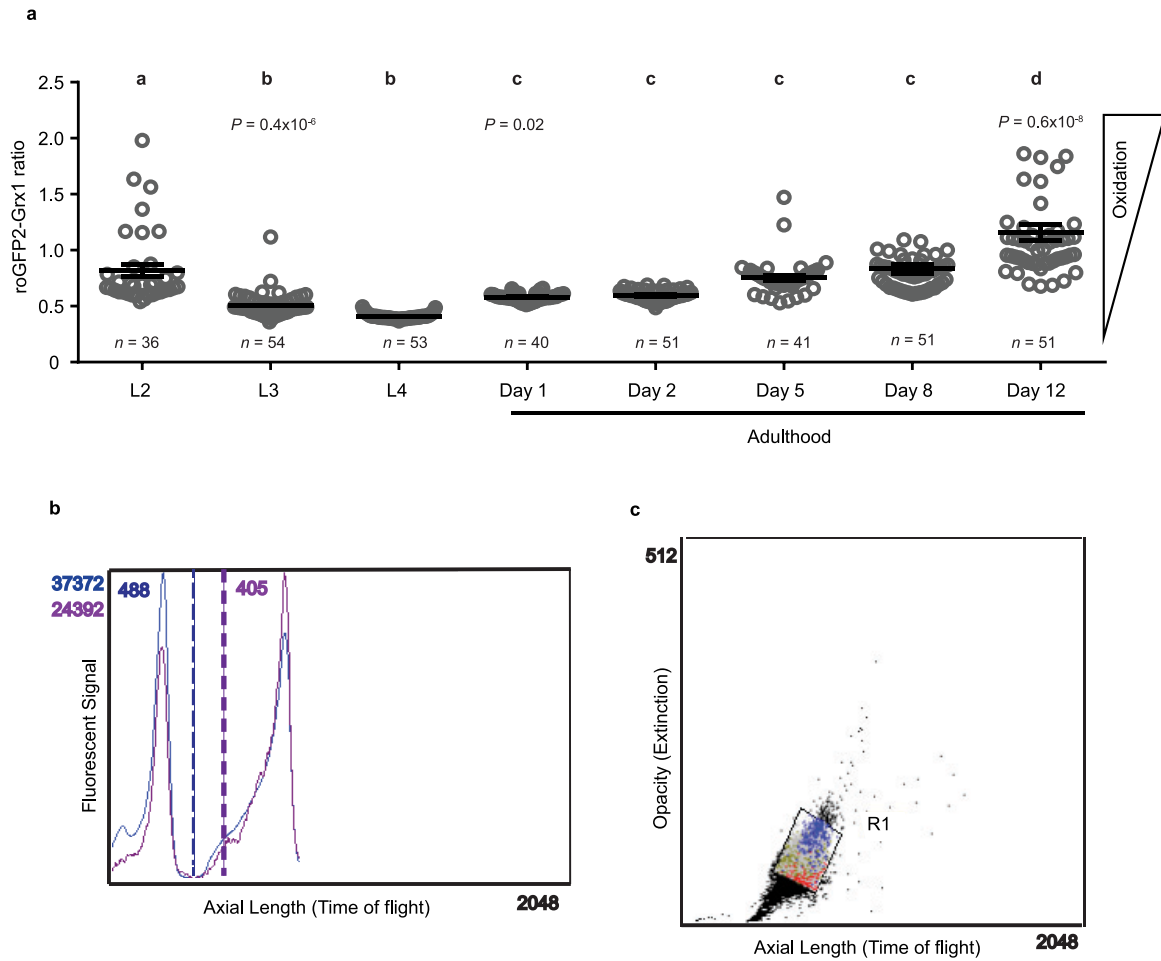
## Additional information

**Supplementary information** is available for this paper at <https://doi.org/10.1038/s41586-019-1814-y>.

**Correspondence and requests for materials** should be addressed to U.J.

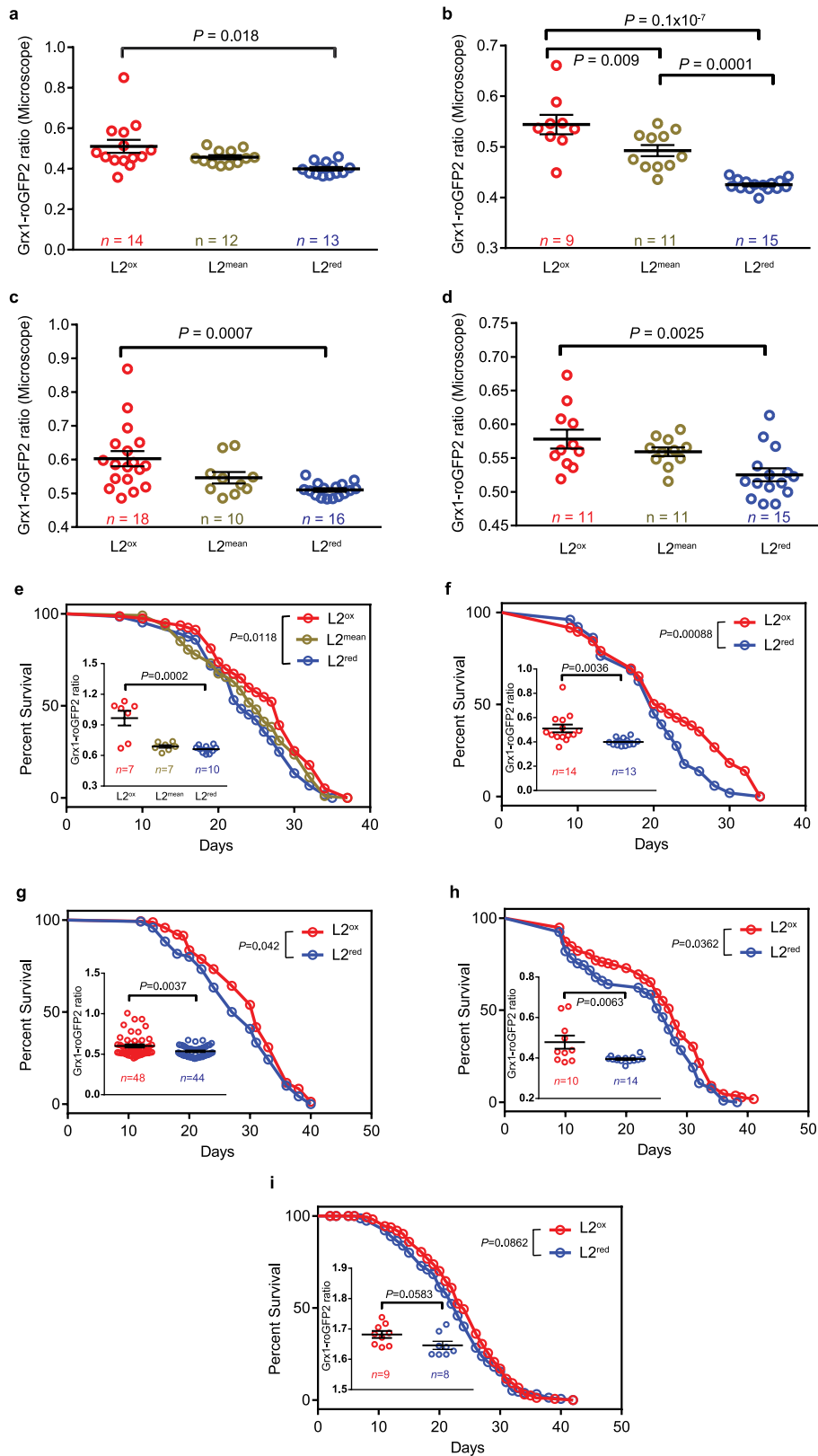
**Peer review information** *Nature* thanks Anne Brunet, Michael Ristow and the other, anonymous, reviewer(s) for their contribution to the peer review of this work.

**Reprints and permissions information** is available at <http://www.nature.com/reprints>.



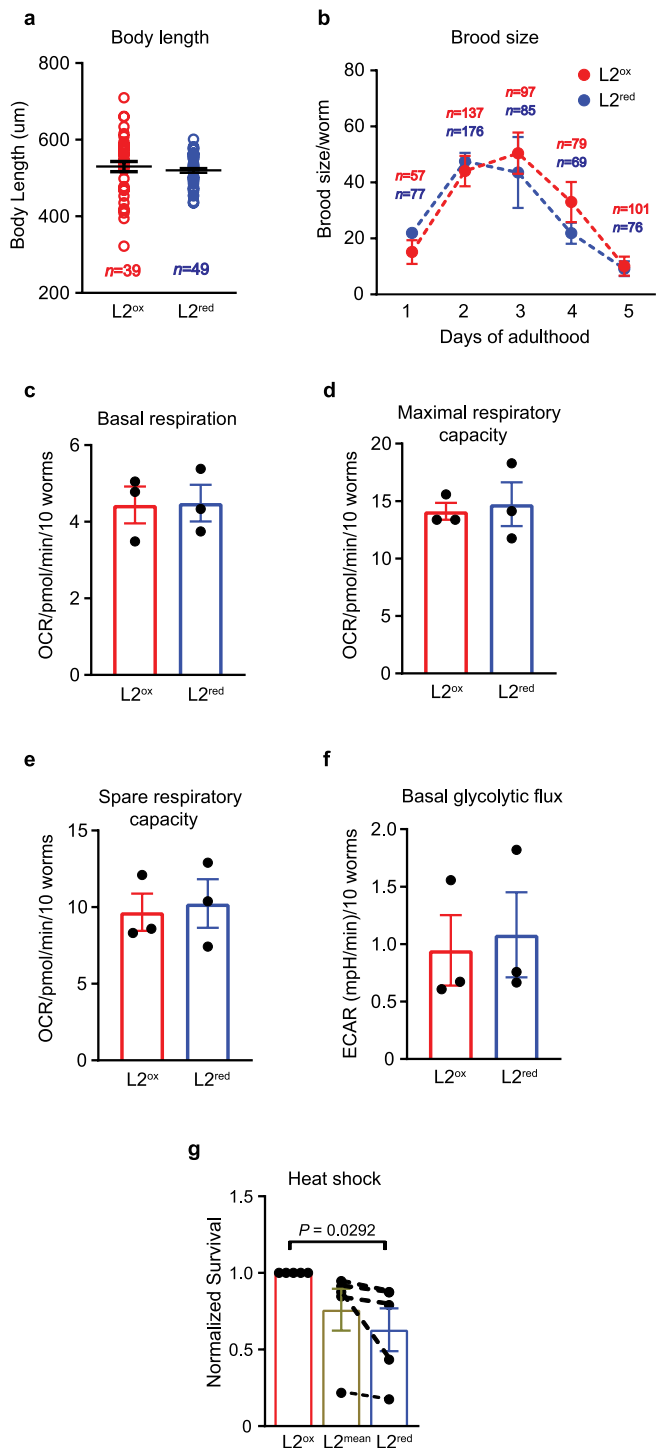
**Extended Data Fig. 1 | In vivo readout of endogenous redox states at different stages during *C. elegans* lifespan and sorting parameters of oxidized and reduced subpopulations. a**, Microscopy analysis of the Grx1-roGFP2 ratio of individual *N2jrls2[Prpl-17::Grx1-roGFP2]* worms (symbol) cultivated at 15 °C and imaged at the indicated time points. Data points that are not significantly different from each other ( $P > 0.05$ ) are labelled with the same

letter. Data are mean  $\pm$  s.e.m;  $n$ , number of worms; one-way ANOVA with Tukey correction. **b**, The Grx-roGFP2 ratio ( $A_{405}/A_{488}$ ) was calculated using the partial profiling feature (pp) configured to analyse extinction and emission data from 488 nm and 405 nm lasers that sequentially excited each worm. **c**, A population of *N2jrls2[Prpl-17::Grx1-roGFP2]* at the L2 stage, separated based on opacity (extinction) and length (time of flight) was gated as R1.

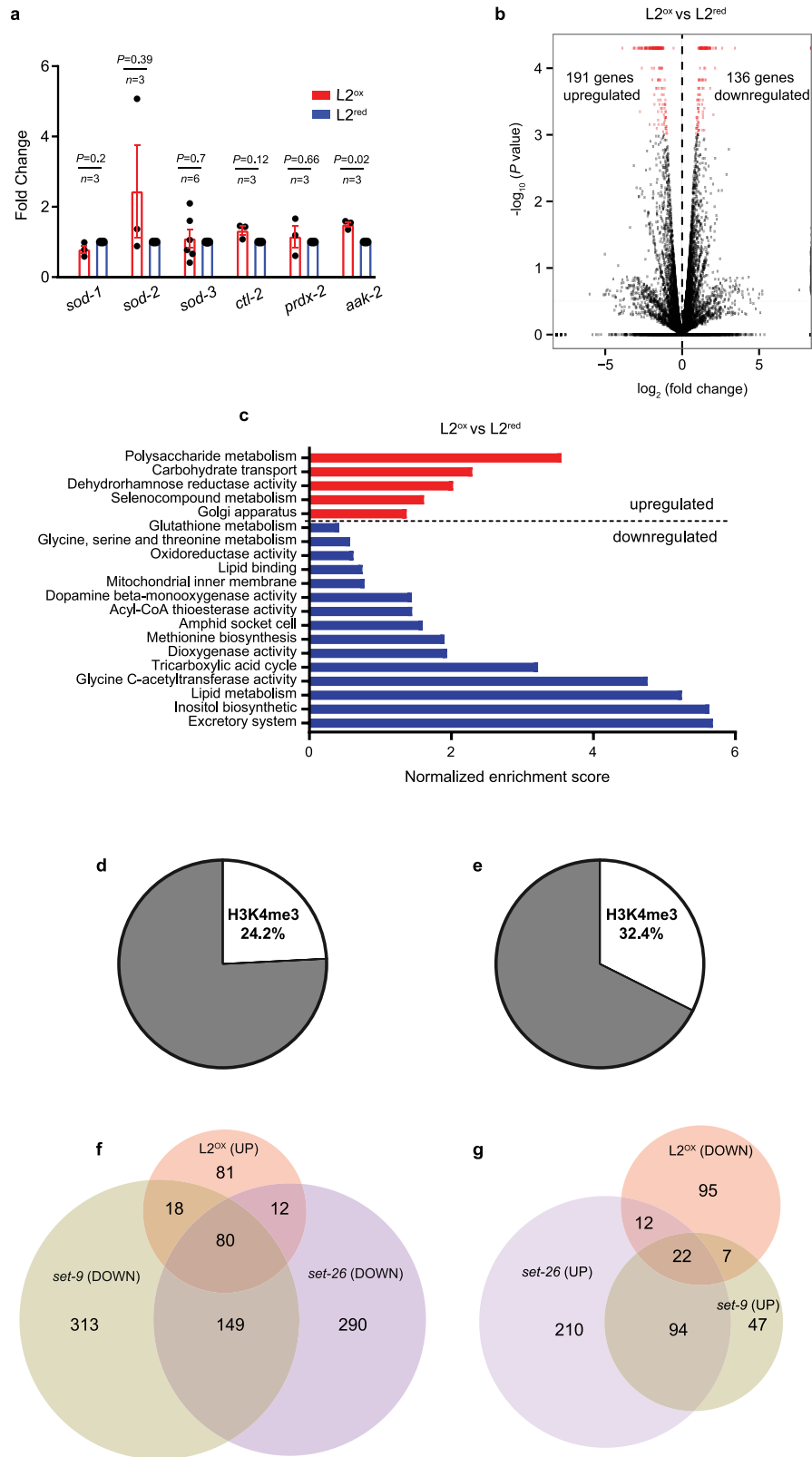


**Extended Data Fig. 2 | Sorting efficiency and lifespan of L2<sup>ox</sup> and L2<sup>red</sup> subpopulations.** **a–d**, Microscopy analysis of the Grx1-roGFP2 ratio of individual worms (dots) previously sorted into L2<sup>ox</sup>, L2<sup>mean</sup> and L2<sup>red</sup> subpopulations.  $n$ , number of worms; one-way ANOVA with Tukey correction. **e–i**, Survival curves of sorted L2<sup>ox</sup>, L2<sup>mean</sup> and L2<sup>red</sup> worms. For  $n$  numbers,

$P$  values (log-rank test) see Extended Data Table 2. Insets, Grx1-roGFP2 ratio of individual worms (dots), assessed by fluorescence microscopy after sorting.  $n$ , number of worms. For  $P$  values (two-sided unpaired  $t$ -test) see Extended Data Table 2.



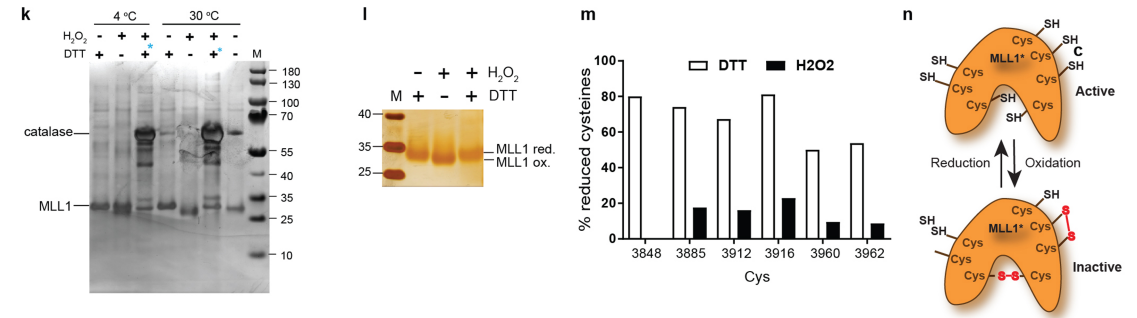
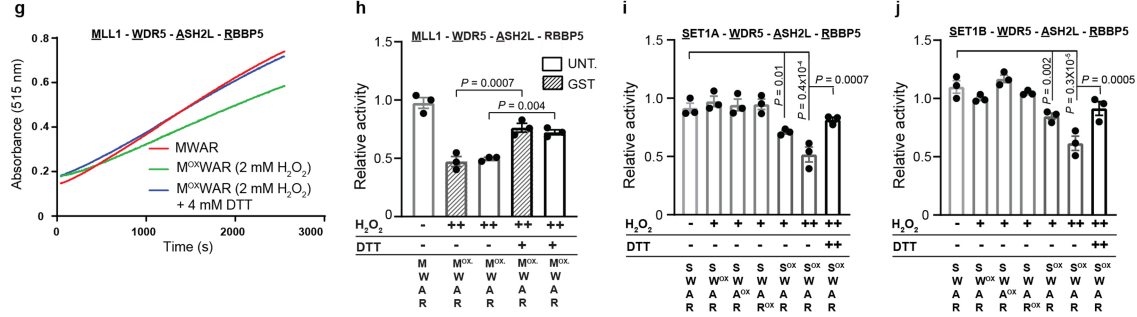
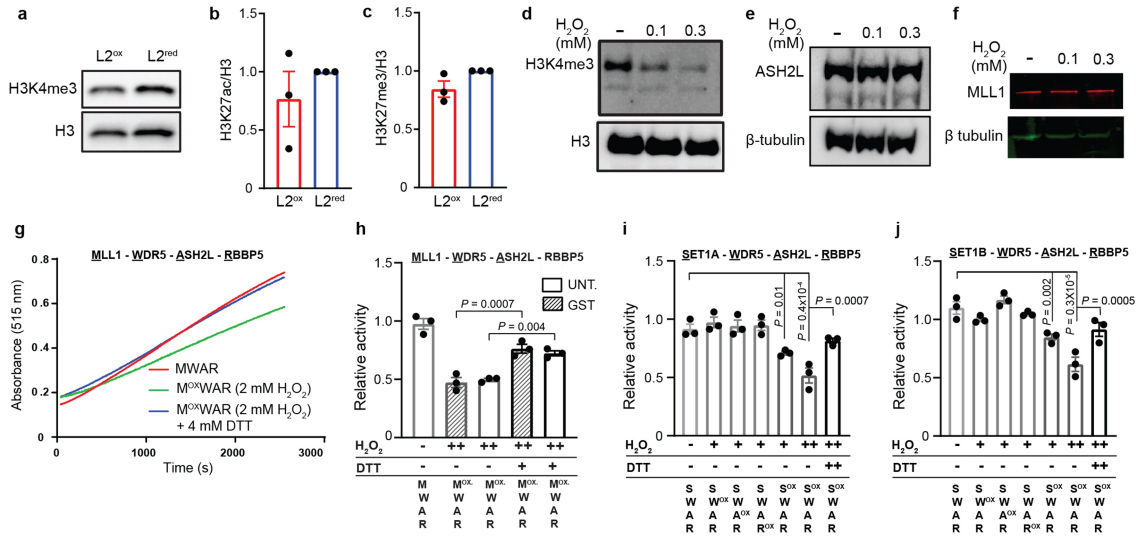
**Extended Data Fig. 3 | Physiological properties of L2<sup>ox</sup> and L2<sup>red</sup> sorted worms.** **a**, Length measurements of L2<sup>ox</sup> and L2<sup>red</sup> worms (symbol) from nose to tail tip immediately after sorting. No significant difference;  $P = 0.4735$  (unpaired two-sided  $t$ -test). **b**, Brood size of L2<sup>ox</sup> and L2<sup>red</sup> worms, measured at the indicated time points.  $n$ , number of worms. No significant difference within a single age;  $P = 0.6532$  (two-way ANOVA). **c–f**, Basal respiration (**c**), maximal (**d**) and spare (**e**) respiratory capacity and basal rates of flux through glycolysis (**f**) of L2<sup>ox</sup> and L2<sup>red</sup> worms.  $n = 3$  independent sorting experiments. ECAR, extracellular acidification rate; OCR, oxygen consumption rate.  $P = 0.9469$  (**c**),  $P = 0.7784$  (**d**),  $P = 0.7904$  (**e**) and  $P = 0.7925$  (**f**); two-sided unpaired  $t$ -test. **g**, Survival of L2<sup>ox</sup>, L2<sup>mean</sup> and L2<sup>red</sup> worms 20 h after heat shock.  $n = 5$  independent sorting experiments; two-sided unpaired  $t$ -test. The connected data points represent data from the same sorting experiment. The survival of L2<sup>ox</sup> is set to 1. All data are mean  $\pm$  s.e.m.



Extended Data Fig. 4 | See next page for caption.

**Extended Data Fig. 4 | Gene expression profiles of L2<sup>ox</sup> and L2<sup>red</sup>.** **a**, Steady-state transcript levels of selected oxidative stress-related genes in L2<sup>ox</sup> and L2<sup>red</sup> worms. *n*, number of independent sorting experiments; unpaired two-sided *t*-test. Data are mean ± s.e.m. **b**, Volcano plot showing fold changes versus *P* values for the transcriptomes of L2<sup>ox</sup> and L2<sup>red</sup> subpopulations. DEGs (*P* ≤ 0.05) are represented by red dots (see Methods for statistical definition of DEGs). Data were collected from four independent sorting experiments. **c**, GSEA of the 327 DEGs. Normalized enrichment scores (see Methods for calculation) are represented by the bar graph. Terms (for summary, see Supplementary Table 1) indicating origin, process or phenotype associated with genes known to have a role in the process are shown on the left. Some terms (\*) have been merged and are represented as a single category bar for

simplicity (for detailed values, see Supplementary Table 1). **d**, **e**, Percentage of DEGs identified in L2<sup>ox</sup> that intersect with H3K4me3 peak signals within their 5' region (500 bp upstream and downstream from the transcription start site). The H3K4me3 chromatin immunoprecipitation (ChIP) datasets were generated from L3-staged N2 worms: ChIP chip, GEO entry GSE30789 in **d** and chromatin immunoprecipitation followed by sequencing (ChIP-seq), GEO entry GSE28770 in **e**, indicating that these marks are set during larval development. Hypergeometric probability: **d**, *P* = 0.064; **e**, *P* = 2.786 × 10<sup>-6</sup>. In **f**, **g**, Venn diagrams show the overlap among upregulated (**f**) or downregulated (**g**) gene sets in L2<sup>ox</sup> and downregulated or upregulated *set-9(rw5)* and *set-26(tm2467)* gene sets (GEO entry: GSE100623). See Supplementary Table 1 for datasets in **d-g**.



**o**

Ce_SET-2	VAAGCSRARPYEKMTMKQKRSVLR--PDNESHPTAIFS--ER-DETAIRHQHLASKDMRL	1344
Hs_SET1A	HQTGSARSEGYYPISSKKEKDKYLDVCPVSARQLE-----G---VDTQGTNRVLSERRS	1538
Hs_SET1B	HVTGCARSEGYYTIDKDKLRYLNSSRASSTDEPPADTQ--GMSIPAQPHASTRAGSERRS	1766
Hs_MLL1	NPHGSARAEVHLRKSADFDMFNFLAS---KHPQPEYNPNDDEEEVQLKS-----	3808
Hs_MLL2	NPHGAARAEVYLRKCTFDMFNFLAS---QHRVLPAGATCDEEEVQLR-----	2550
Hs_MLL3	NPTGCARSEPKMSAHVKRF--VLRPHLNTSTSKSFQSTVT--G-----	4744
Hs_MLL4	NPTGCARSEPKLITHYK-----RPHTLNTSMKAYQSTFT--GETNTPY-----	5376

Ce_SET-2	LQRLLTSLG---DANNDFKINQLKFRKKMKIFARSRIHGWLGYAMESIAPDEMIVEYI	1401
Hs_SET1A	EQRRLLSAGTSAIMSDLLKLNQLKFRKKLFRGRSRIHEWGLFAMEPIAADMVIEYV	1598
Hs_SET1B	EQRRLLSFTG--SCDSLLKFNQLKFRKKLKFCKSHIDWGLFAMEPIAADMVIEYV	1857
Hs_MLL1	--ARRATSMPLPMPMR---FRHLKKTKEAVGVYRSPIHGRGLFCKRNIADGEMVIEYA	3862
Hs_MLL2	-----STHLKKTKEAVGVYRSPIHGRGLFCKRNIADGEMVIEYS	2605
Hs_MLL3	-----KMKTEWKSNNVYLARSRIQGLGLYAAKDIKHTMVEYI	4801
Hs_MLL4	--SKQFVHS-----KSSQYRRLRTEWKNNVYLARSRIQGLGLYAAKDIKHTMVEYI	5427

Ce_SET-2	GQTIRSLVAEEREKAYERRIGSSYLFRIDLHHVIDATKRGNFARFINHSCQPNCYAKVL	1461
Hs_SET1A	GQNIRQVMADMREKRYVQEGIGSSYLFRVDHDTIIDATKCGNLFARFINHCTPNCYAKVI	1658
Hs_SET1B	GQNIRQVIADMREKRYVDEGIGSSYMFVRVDHDTIIDATKCGNLFARFINHSCNPNCYAKVI	1917
Hs_MLL1	GNVIRSIQTDKREKYDCKGIG-CYMFRIIDSEVVDATMHGNAARFINHSCPNCSRVI	3921
Hs_MLL2	GIVIRSVLTKREKFDGKIG-CYMFRRMDFVDVVDATMHGNAARFINHSCPNCSRVI	2664
Hs_MLL3	GTIIRNEVANRREKLYESQNRG-VYMFRRMNDHVIDATLTGGPARYINHSCAPNCVAEVV	4860
Hs_MLL4	GTIIRNEVANRREKIYEEQNRG-IYMFRIINNEHVIDATLTGGPARYINHSCAPNCVAEVV	5486

Ce_SET-2	TIEGKRVIVISRTIIKKGEETIYDYKFFIED--DKIDCLGAKTIRGYLN	1510
Hs_SET1A	TIESQKKIVISKQPIGVDEEITDYKFFLED--NKIPCLGTESTRGLN	1707
Hs_SET1B	TVESQKKIVISKQHINVEEITDYKFFIED--VKIPCLGSENGRGLN	1966
Hs_MLL1	NIDGQKHIVIFAMRKIYRGEELTYDYKFFIEDASNKLPNCGAKKCRFLN	3972
Hs_MLL2	HVEGQKHIVIFALRRILRGEELTYDYKFFIEDASNKLPNCGAKKCRFLN	2715
Hs_MLL3	TFERGHKIIISSRRIPKGEELTYDYKFFIEDDQHKIPCHGAVNCRKWMN	4911
Hs_MLL4	TFDKEDIIISSRRIPKGEELTYDYKFFIEDDQHKIPCHGAVNCRKWMN	5537

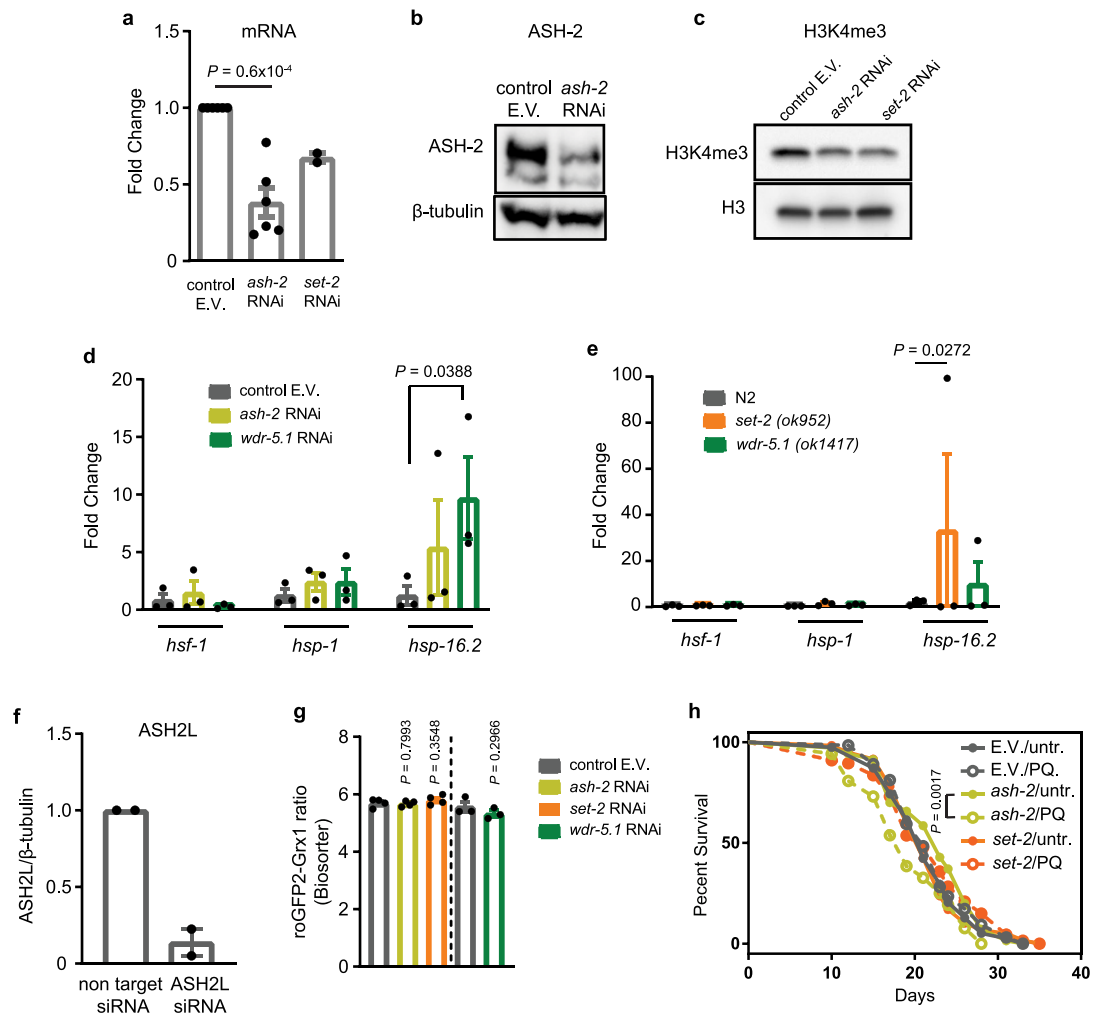
  

Ce\_SET-2, *C. elegans* (NP\_498039.1)  
Hs\_SET1A, Homo sapiens SETD1A (NP\_055527.1)  
Hs\_SET1B, Homo sapiens SETD1B (NP\_01340274.1)  
Hs\_MLL1, Homo sapiens KMT2A (NP\_001184033.1)  
Hs\_MLL2, Homo sapiens KMT2B (NP\_055542.1)  
Hs\_MLL3, Homo sapiens KMT2C (NP\_733751.2)  
Hs\_MLL4, Homo sapiens KMT2D (NP\_003473.3)

Extended Data Fig. 5 | See next page for caption.

**Extended Data Fig. 5 | Redox sensitivity of in vivo H3K4me3 levels and in vitro histone methyltransferase complex activity.** **a**, Global H3K4me3 levels in the sorted L2<sup>ox</sup> and L2<sup>red</sup> worms. A representative western blot using antibodies against H3K4me3 is shown. **b, c**, Quantification of global H3K27ac (**b**) and H3K27me3 (**c**) levels by western blot.  $n = 3$  independent sorting experiments.  $P = 0.3793$  (**b**) and  $P = 0.0905$  (**c**); unpaired two-sided  $t$ -test. Data represent mean  $\pm$  s.e.m. **d-f**, Global H3K4me3 (**d**), ASH2L (**e**) and MLL1 (**f**) levels in HeLa cells before and after H<sub>2</sub>O<sub>2</sub> treatment, as assessed by western blot. **g**, Time course of the in vitro methyltransferase reaction for core COMPASS subunits (SET domain of MLL1-WDR5-ASH2L-RBBP5). Reaction rates were derived from the first 20 min of the linear range. **h-j**, In vitro histone methyltransferase assays of core COMPASS subunits, consisting of purified GST-WDR5 (WDR5), GST-ASH2L (ASH2L), GST-RBBP5 (RBBP5) and either GST-MLL1 SET domain or untagged MLL1 SET domain (**h**), GST-SET1A SET domain (**i**) or GST-SET1B SET domain (**j**). Superscript ox indicates that the protein was pre-treated with either 1 mM (+) or 2 mM (++) H<sub>2</sub>O<sub>2</sub> for 30 min before the activity assay. DTT was added after the H<sub>2</sub>O<sub>2</sub> treatment.  $n = 3$  independent experiments; one-way ANOVA with Sidak correction. Data are mean  $\pm$  s.e.m. **k**, The MLL1 SET

domain was treated with either 2 mM DTT, 2 mM H<sub>2</sub>O<sub>2</sub> or 2 mM H<sub>2</sub>O<sub>2</sub>, followed by 4 mM DTT. Catalase was used to quench the H<sub>2</sub>O<sub>2</sub>. The proteins were denatured and thiols were modified with NEM before loading onto non-reducing SDS-PAGE to prevent non-specific thiol oxidation. The proteins were visualized by silver staining. **M**, marker. **l**, MLL1 SET domain treated with either 2 mM DTT, 2 mM H<sub>2</sub>O<sub>2</sub> or 2 mM H<sub>2</sub>O<sub>2</sub>, followed by 4 mM DTT. All reduced protein thiols were then labelled with the 500-Da thiol-reactive compound AMS, causing a 500-Da mass decrease per oxidized thiol—detectable on reducing SDS-PAGE. **M**, protein marker. **m**, Cysteine oxidation state in MLL1 SET domain after treatment with either 2 mM DTT or 2 mM H<sub>2</sub>O<sub>2</sub> followed by NEM labelling as assessed by LC-MS/MS. The peptide containing Cys3967 could not be detected. **n**, Schematic representation of the redox sensitivity of the MLL1 SET domain. For blot and gel source images, see Supplementary Figs. 1 and 3. **o**, Sequence alignment of the SET domain. All cysteines in MLL1 are shown in bold, and the five absolutely conserved cysteines are highlighted in yellow. Cysteines shown to be involved in zinc coordination are marked with an asterisk. NCBI protein BLAST and Clustal Omega Multiple Sequence Alignment, Clustal O (1.2.4) were used.



**Extended Data Fig. 6 | Effects of H3K4me3 downregulation on heat-shock response and endogenous redox state.** **a**, ASH-2 and SET-2 transcript levels of *N2jrls2[Prpl-17::Grx1-roGFP2]* worms treated with *ash-2* or *set-2* RNAi for 2 generations.  $n = 6$  (*ash-2*) and  $n = 2$  (*set-2*) independent experiments; unpaired two-sided *t*-test. E.V., empty vector. **b**, ASH-2 protein levels in *N2jrls2[Prpl-17::Grx1-roGFP2]* worms treated with control RNAi or *ash-2* RNAi for two generations using western blot analysis. **c**, H3K4me3 levels in *N2jrls2[Prpl-17::Grx1-roGFP2]* worms treated with control RNAi, *ash-2* RNAi or *set-2* RNAi for two generations. **d**, Transcript levels of selected heat-shock genes after heat-shock treatment of *N2jrls2[Prpl-17::Grx1-roGFP2]* worms treated with the indicated RNAi.  $n = 3$  independent experiments; one-way ANOVA with Bonferroni correction. **e**, Transcript levels of selected heat-shock

genes in *set-2* or *wdr-5.1* mutants before and after heat-shock treatment.  $n = 3$  independent experiments; one-way ANOVA with Bonferroni correction. **f**, ASH2L levels following ASH2L siRNA treatment of HeLa cells.  $n = 2$  independent experiments. **g**, Grx1-roGFP2 ratios of L2 larval worms treated with *ash-2* RNAi, *set-2* RNAi, *wdr-5.1* RNAi or the empty vector were measured using the BioSorter.  $n = 4$  (*ash-2*, *set-2*) and  $n = 3$  (*wdr-5.1*) independent sorting experiments; unpaired two-sided *t*-test. **h**, Representative survival curves of *N2jrls2[Prpl-17::Grx1-roGFP2]* worms treated with *ash-2* or *set-2* RNAi for two generations and treated with 1 mM paraquat (PQ) for 10 h at the L2 larval stage. For  $n$  numbers, repetitions and statistics (log-rank), see Extended Data Table 4. Data in **a**, **d**–**g**, represent mean  $\pm$  s.e.m. For blot source images, see Supplementary Figs. 1, 3.

**Extended Data Table 1 | Lifespan assays of L2<sup>ox</sup>, L2<sup>mean</sup> and L2<sup>red</sup> subpopulations following heat-shock treatment or in the continuous presence of paraquat or juglone**

Condition	Experiment	Sorted population	Mean	Max	Dead/ censored worms	P value	% change	Figure on text	Ratio BioSorter <sup>‡</sup>	P value (BioS.)
Heat shock (long term)	1	L2 <sup>ox</sup>	19	32.5	24				7.44±0.01(n=238)	
		L2 <sup>mean</sup>	17	31.5	19/4	0.639	10.5%*	Figure 2a	7.37±0.02(n=135)	0.002
		L2 <sup>red</sup>	13	27.3	32/1	0.0088	31.6%*		7.29±0.02(n=132)	0.2x10 <sup>-8</sup>
	2	L2 <sup>ox</sup>	17.5	25	29/13				7.06±0.01(n=698)	
		L2 <sup>red</sup>	12	21	20/3	0.0077	31.4%*	7.01±0.012(n=319)	0.002	
	3	L2 <sup>ox</sup>	18	25.9	96/2			7.15±0.007(n=893)		
L2 <sup>red</sup>		15	24.2	77/1	0.0153	16.7%*	7.12±0.012(n=914)	0.009		
Paraquat (2 mM)	1	L2 <sup>ox</sup>	17	26	13				7.09±0.02(n=116)	
		L2 <sup>mean</sup>	14	26	11	0.4456	17.6%*	Figure 2b	6.99±0.033(n=113)	0.006
		L2 <sup>red</sup>	10	21	20	0.0215	41.2%*		6.67±0.045(n=108)	0.2x10 <sup>-13</sup>
	2	L2 <sup>ox</sup>	13	18.5	38				7.35±0.017(n=158)	
		L2 <sup>red</sup>	11	18.5	40	0.0456	15.4%*	7.14±0.011(n=277)	0.1x10 <sup>-19</sup>	
	3	L2 <sup>ox</sup>	13	18.6	47			6.71±0.02(n=139)		
L2 <sup>red</sup>		12	15.5	38	0.0037	16.7% <sup>†</sup>	6.33±0.06(n=100)	0.8x10 <sup>-7</sup>		
Juglone (250 μM)	1	L2 <sup>ox</sup>	23	32.4	72				6.59±0.012(n=428)	
		L2 <sup>red</sup>	19	32.4	73	0.0033	17.4%*	6.55±0.012(n=513)	0.007	
	2	L2 <sup>ox</sup>	18	33.3	86			7.43±0.01(n=186)		
		L2 <sup>red</sup>	18	29.5	59	0.0202	11.4% <sup>†</sup>	7.27±0.015(n=161)	0.1x10 <sup>-16</sup>	

Worms were sorted onto NGM plates and exposed to heat-shock treatment or the indicated compounds. P values for Kaplan–Meier survival analysis were calculated on the basis of the log-rank (Mantel–Cox) method. Samples were compared with L2<sup>ox</sup> subpopulations. Maximum lifespan was defined as the lifespan of the last 10% of the population.

\*Percentage change based on mean lifespan.

<sup>†</sup>Percentage change based on maximum lifespan.

<sup>‡</sup>Grx1-roGFP2 ratio of L2<sup>ox</sup> and L2<sup>red</sup> subpopulations, based on BioSorter analysis during sorting. Data are mean ± s.e.m. n, number of worms. Two-sided unpaired t-test.

# Article

**Extended Data Table 2 | Lifespan assays of L2<sup>ox</sup>, L2<sup>mean</sup> and L2<sup>red</sup> subpopulations**

Exp.	Sorted population	Mean	Max	Dead/ censored worms	P value (survival)	% change	Figure on text	Ratio BioSorter <sup>§</sup>	P value (BioS.)	Ratio Microscope <sup>  </sup>	P value (Micr.)
1	L2 <sup>ox</sup>	30	35.8	97				6.88±0.02(n=134)		0.49±0.008(n=36)	
	L2 <sup>mean</sup>	26	33.5	74	0.007	13.3%*	Fig. 2c	6.69±0.02(n=143)	0.1×10 <sup>-8</sup>	0.45±0.003(n=49)	0.1×10 <sup>-6</sup>
	L2 <sup>red</sup>	25	32.3	58	0.0004	17%*		6.62±0.04(n=131)	0.4×10 <sup>-6</sup>	0.44±0.003(n=50)	0.1×10 <sup>-7</sup>
2	L2 <sup>ox</sup>	28	35.1	78/2				7.14±0.02(n=127)		0.96±0.07(n=7)	
	L2 <sup>mean</sup>	25	34.3	105/3	0.1018	10.7%*		7.11±0.03(n=133)	0.532	0.69±0.01(n=7)	0.0027
	L2 <sup>red</sup>	23	33.5	63/1	0.0118	17.8%*		6.94±0.07(n=136)	0.0101	0.66±0.01(n=10)	0.0002
3	L2 <sup>ox</sup>	21	34	94/2				7.45±0.02(n=139)		0.51±0.03(n=14)	
	L2 <sup>red</sup>	20	30	51	0.0088	12% <sup>†</sup>		7.35±0.01(n=716)	0.0003	0.45±0.01(n=13)	0.0036
4	L2 <sup>ox</sup>	31	39.4	162/3				6.61±0.02(n=170)		0.6±0.02(n=48)	
	L2 <sup>red</sup>	28.5	38.8	120	0.042	8%*		6.55±0.02(n=161)	0.0456	0.54±0.01(n=44)	0.0037
5	L2 <sup>ox</sup>	28	36	114/4				7.29±0.01(n=191)		0.48±0.03(n=10)	
	L2 <sup>red</sup>	26	35.4	106	0.0362	7%*		7.12±0.02(n=88)	0.3×10 <sup>-9</sup>	0.39±0.004(n=14)	0.0063
6 <sup>¶</sup>	L2 <sup>ox</sup>	24	34	164/7				6.19±0.02(n=275)		1.68±0.01(n=9)	
	L2 <sup>red</sup>	23	34	155/9	0.0862 <sup>‡</sup>	4%*		6.03±0.02(n=273)	0.5×10 <sup>-7</sup>	1.65±0.01(n=8)	0.0583
7	E.V. <sup>ox</sup>	24	34	46				5.55±0.04(n=114)			
	E.V. <sup>red</sup>	21	28.3	63	0.0004	12.5%*	Fig. 4d	4.49±0.067(n=114)	0.5×10 <sup>-28</sup>		
8	E.V. <sup>ox</sup>	24	33	77/3				6.37±0.035(n=60)			
	E.V. <sup>red</sup>	20	31	80	0.002	17%*	Fig. 4e	5.85±0.076(n=63)	0.1×10 <sup>-7</sup>		
9	E.V. <sup>ox</sup>	20	33	85				6.08±0.046(n=133)			
	E.V. <sup>red</sup>	17	30.7	77	0.0264	15%*		5.87±0.052(n=107)	0.0032		
10	E.V. <sup>ox</sup>	18	28.7	89/1				6.03±0.022(n=225)			
	E.V. <sup>red</sup>	18	25.4	85	0.0077	11.5% <sup>†</sup>		5.10±0.038(n=226)	0.3×10 <sup>-62</sup>		

Worms were sorted onto NGM plates and assessed for lifespan. P values for Kaplan–Meier survival analysis were calculated on the basis of the log-rank (Mantel–Cox) method unless noted otherwise. Samples were compared with L2<sup>ox</sup> subpopulations. Maximum lifespan was defined as the lifespan of the last 10% of the population. E.V., empty vector (control RNAi conditions for experiments in Extended Data Table 4).

\*Percentage change based on mean lifespan.

<sup>†</sup>Percentage change based on maximum lifespan.

<sup>‡</sup>P value for survival analysis calculated based on the Gehan–Breslow–Wilcoxon method.

<sup>§</sup>Grx1–roGFP2 ratio of L2<sup>ox</sup> and L2<sup>red</sup> subpopulations, based on BioSorter analysis during sorting. Data represent mean ± s.e.m. n, number of worms. Two-sided unpaired t-test.

<sup>||</sup>Grx1–roGFP2 ratio of L2<sup>ox</sup> and L2<sup>red</sup> subpopulations based on microscopy analysis, following sorting. Data are mean ± s.e.m. n, number of worms. Two-sided unpaired t-test.

<sup>¶</sup>Lifespan assay conducted with experimenter blind to the type of worms assayed.

**Extended Data Table 3 | Lifespan assays of L2<sup>ox</sup> and L2<sup>red</sup> subpopulations following transient exposure to oxidizing or reducing conditions**

Experiment	Sorted population	Mean	Max	Dead/ censored worms	P value	% change	Figure on text	Ratio BioSorter <sup>§</sup>	P value (BioS.)
1	L2 <sup>ox</sup>	24	34.4	91				7.07±0.018(n=317)	
	1 mM PQ	26	33.7	85	0.4364	7.7%*	Figure 2f		
	10 mM NAC	19	32.9	99	0.008	20.8%*			
	L2 <sup>red</sup>	21	31.2	109				7.±0.011(n=402)	0.00074
	1 mM PQ	23	31.7	139/1	0.0261	8.7%*	Figure 2e		
	10 mM NAC	21	29.4	157	0.0546	-			
2	L2 <sup>ox</sup>	16	23.3	86				7.09±0.007(n=800)	
	L2 <sup>red</sup>	15	19	54	0.0002	18.4% <sup>†</sup>		7.05±0.009(n=1218)	0.00034
	L2 <sup>red</sup> + 1 mM PQ	15.5	25.6	64	0.0002 <sup>‡</sup>	9% <sup>†</sup>			
3	L2 <sup>ox</sup>	23	29.8	89					
	10 mM NAC	21	30.4	50	0.05 <sup>‡</sup>	8.7%*			
4 <sup>¶</sup>	L2 <sup>Mixed</sup>	15	21.1	66					
	0.1 mM PQ	15	20.6	107	0.5137	2.4% <sup>†</sup>	Figure 2d		
	1 mM PQ	15	27.8	96	0.0175	24.1% <sup>†</sup>			
	10 mM NAC	14.5	19.5	66	0.3667	7.6% <sup>†</sup>			
5 <sup>¶</sup>	L2 <sup>Mixed</sup>	12	16	84					
	0.1 mM PQ	12	20.7	101	0.003	22.7% <sup>†</sup>			
	1 mM PQ	12	29.7	88	0.0023	46.1% <sup>†</sup>			
	10 mM NAC	11	18.7	101	0.1809	14.4% <sup>†</sup>			

Worms were sorted into liquid medium, exposed to paraquat or NAC for 10 h and then returned to NGM plates for lifespan assessment. P values for Kaplan–Meier survival analysis were calculated on the basis of the log-rank (Mantel–Cox) method unless noted otherwise. Samples were compared with L2<sup>ox</sup> subpopulations or L2<sup>Mixed</sup> populations. Maximum lifespan was defined as the lifespan of the last 10% of the population.

\*Percentage change based on mean lifespan.

<sup>†</sup>Percentage change based on maximum lifespan.

<sup>‡</sup>P value for survival analysis calculated based on the Gehan–Breslow–Wilcoxon method.

<sup>§</sup>Grx1-roGFP2 ratio of L2<sup>ox</sup> and L2<sup>red</sup> subpopulations at the L2 stage, based on BioSorter analysis during sorting. Data are mean ± s.e.m. n, number of worms. Two-sided unpaired t-test.

<sup>¶</sup>Sample compared with the reduced subpopulation.

<sup>¶</sup>Lifespan assays performed in the lifespan machine (see Methods).

## Extended Data Table 4 | Lifespan assays upon H3K4me3-targeting RNAi treatment

Exp.	Sorted population	Mean	Max	Dead/ censored worms	P value	% change	Figure on text	Ratio BioSorter <sup>‡</sup>	P value (BioS.)
1 <sup>&amp;</sup>	<i>ash-2</i> RNAi <sup>ox</sup>	24	33.3	40/2			Figure 4d	5.00±0.043(n=95)	
	<i>ash-2</i> RNAi <sup>red</sup>	25	34	45/4	0.1373	4.2%*		4.66±0.046(n=85)	0.1x10 <sup>-6</sup>
2 <sup>&amp;</sup>	<i>set-2</i> RNAi <sup>ox</sup>	22	32	57/1			Figure 4e	6.17±0.047(n=52)	
	<i>set-2</i> RNAi <sup>red</sup>	22	30	72/1	0.7739	-		5.64±0.03(n=224)	0.2x10 <sup>-14</sup>
3 <sup>&amp;</sup>	<i>ash-2</i> RNAi <sup>ox</sup>	30	39.1	70				6.12±0.03(n=186)	
	<i>ash-2</i> RNAi <sup>red</sup>	30	37.1	79	0.5721	-		5.8±0.039(n=216)	0.9x10 <sup>-9</sup>
	<i>set-2</i> RNAi <sup>ox</sup>	20	34	76				6.13±0.019(n=259)	
	<i>set-2</i> RNAi <sup>red</sup>	20	33	55	0.7339	-		5.67±0.026(n=295)	0.1x10 <sup>-38</sup>
4 <sup>&amp;</sup>	<i>ash-2</i> RNAi <sup>ox</sup>	25	30.2	87				6.17±0.021(n=223)	
	<i>ash-2</i> RNAi <sup>red</sup>	25	30.4	79	0.9133	-		5.56±0.046(n=223)	0.5x10 <sup>-26</sup>
	<i>set-2</i> RNAi <sup>ox</sup>	18	25.7	76				6.19±0.025(n=214)	
	<i>set-2</i> RNAi <sup>red</sup>	18	27	85	0.8589	4.8% <sup>†</sup>		5.29±0.041(n=217)	0.1x10 <sup>-52</sup>
5	control E.V. untr.	21	30	78			Ext. Data Fig. 6h		
	control E.V. PQ	21	31.7	64	0.5073	-			
	<i>ash-2</i> RNAi untr.	23	30.4	70					
	<i>ash-2</i> RNAi PQ	19	27.6	52	0.0017	17.4%*			
	<i>set-2</i> RNAi untr.	21	31.3	59					
	<i>set-2</i> RNAi PQ	21	32.1	67	0.4515	-			
6	control E.V. untr.	20	29.5	58					
	control E.V. PQ	18	32.3	43	0.7952	10%*			
	<i>ash-2</i> RNAi untr.	23	31.4	46					
	<i>ash-2</i> RNAi PQ	17	32.3	30	0.3873	26%*			
	<i>set-2</i> RNAi untr.	20	28.8	47					
	<i>set-2</i> RNAi PQ	23	28.7	39	0.3225	13%*			

Worms were treated with the indicated RNAi and sorted into L2<sup>ox</sup> and L2<sup>red</sup> at the F<sub>2</sub> generation (experiments 1–4).

<sup>&</sup>The corresponding empty-vector controls for experiments 1–4 are shown in Extended Data Table 1 experiments 7–10. Worms were treated with 1 mM paraquat for 10 h at the L2 stage following RNAi treatment with *ash-2* or *set-2* (experiments 5 and 6). P values for Kaplan–Meier survival analysis were calculated on the basis of the log-rank (Mantel–Cox) method. Samples were compared with the respective L2<sup>ox</sup> or untreated control. Maximum lifespan was defined as the lifespan of the last 10% of the population.

\*Percentage change based on mean lifespan.

<sup>†</sup>Percentage change based on maximum lifespan.

<sup>‡</sup>Grx1-roGFP2 ratio of L2<sup>ox</sup> and L2<sup>red</sup> subpopulations, based on BioSorter analysis during sorting. Data are mean ± s.e.m. n, number of worms. Two-sided unpaired t-test.

## Reporting Summary

Nature Research wishes to improve the reproducibility of the work that we publish. This form provides structure for consistency and transparency in reporting. For further information on Nature Research policies, see [Authors & Referees](#) and the [Editorial Policy Checklist](#).

### Statistics

For all statistical analyses, confirm that the following items are present in the figure legend, table legend, main text, or Methods section.

n/a Confirmed

- The exact sample size ( $n$ ) for each experimental group/condition, given as a discrete number and unit of measurement
- A statement on whether measurements were taken from distinct samples or whether the same sample was measured repeatedly
- The statistical test(s) used AND whether they are one- or two-sided  
*Only common tests should be described solely by name; describe more complex techniques in the Methods section.*
- A description of all covariates tested
- A description of any assumptions or corrections, such as tests of normality and adjustment for multiple comparisons
- A full description of the statistical parameters including central tendency (e.g. means) or other basic estimates (e.g. regression coefficient) AND variation (e.g. standard deviation) or associated estimates of uncertainty (e.g. confidence intervals)
- For null hypothesis testing, the test statistic (e.g.  $F$ ,  $t$ ,  $r$ ) with confidence intervals, effect sizes, degrees of freedom and  $P$  value noted  
*Give  $P$  values as exact values whenever suitable.*
- For Bayesian analysis, information on the choice of priors and Markov chain Monte Carlo settings
- For hierarchical and complex designs, identification of the appropriate level for tests and full reporting of outcomes
- Estimates of effect sizes (e.g. Cohen's  $d$ , Pearson's  $r$ ), indicating how they were calculated

*Our web collection on [statistics for biologists](#) contains articles on many of the points above.*

### Software and code

Policy information about [availability of computer code](#)

Data collection  
BioRad - Image Lab (v5.2.1) was used for collecting gel and blot images  
Union Biometrica - FlowPilot v. 1.5.9.4 was used to collect and analyze Biosorter data  
No software or computer code was used to generate data

Data analysis  
Prism - GraphPad Software Inc. (v7.0c)  
Fiji - ImageJ (v1.52a) bundled with Java 1.8.0\_112  
Microsoft Office 2010 Excel  
FastQC (version v0.11.3)  
TopHat (version 2.0.13)  
Bowtie2 (version 2.2.1.)  
Cufflinks/CuffDiff (version 2.1.1)  
CummeRbund R  
Bioconductor Package GSA

For manuscripts utilizing custom algorithms or software that are central to the research but not yet described in published literature, software must be made available to editors/reviewers. We strongly encourage code deposition in a community repository (e.g. GitHub). See the Nature Research [guidelines for submitting code & software](#) for further information.

### Data

Policy information about [availability of data](#)

All manuscripts must include a [data availability statement](#). This statement should provide the following information, where applicable:

- Accession codes, unique identifiers, or web links for publicly available datasets
- A list of figures that have associated raw data
- A description of any restrictions on data availability

RNA-sequencing data described in this study have been uploaded to the Gene Expression Omnibus (GEO) database with accession number GSE138502 and will be

made public upon publication.

Source data files as well as uncropped gel and blot images are provided with the paper. Supplementary Table 1 contains RNAseq data and analysis.

## Field-specific reporting

Please select the one below that is the best fit for your research. If you are not sure, read the appropriate sections before making your selection.

Life sciences  Behavioural & social sciences  Ecological, evolutionary & environmental sciences

For a reference copy of the document with all sections, see [nature.com/documents/nr-reporting-summary-flat.pdf](https://www.nature.com/documents/nr-reporting-summary-flat.pdf)

## Life sciences study design

All studies must disclose on these points even when the disclosure is negative.

Sample size	No sample-size calculations were performed. Sample size was determined to be adequate based on the magnitude and consistency of measurable differences between groups in preliminary experiments. RNA sequencing was performed in 4 biological replicates. The very high correlation between these replicates suggests that this is sufficient. In many experiments numerous worms were available and large sample sizes were used.
Data exclusions	In lifespan assays, we excluded plates based on the following pre-established criteria: 1) growth of bacteria that were not originally seeded on the plate 2) fungal growth 3) plate desiccation.
Replication	All findings reported were reliably reproduced in the lab on independent occasions : 1) different facilities 2) different C. elegans stocks 3) un
Randomization	Samples were allocated into groups (oxidized vs reduced) based on Grx1-roGFP2 readouts using a large - particle flow cytometer i.e. BioSorter
Blinding	Blinding was performed on lifespan assays

## Reporting for specific materials, systems and methods

We require information from authors about some types of materials, experimental systems and methods used in many studies. Here, indicate whether each material, system or method listed is relevant to your study. If you are not sure if a list item applies to your research, read the appropriate section before selecting a response.

### Materials & experimental systems

n/a	Involved in the study
<input type="checkbox"/>	<input checked="" type="checkbox"/> Antibodies
<input type="checkbox"/>	<input checked="" type="checkbox"/> Eukaryotic cell lines
<input checked="" type="checkbox"/>	<input type="checkbox"/> Palaeontology
<input type="checkbox"/>	<input checked="" type="checkbox"/> Animals and other organisms
<input checked="" type="checkbox"/>	<input type="checkbox"/> Human research participants
<input checked="" type="checkbox"/>	<input type="checkbox"/> Clinical data

### Methods

n/a	Involved in the study
<input checked="" type="checkbox"/>	<input type="checkbox"/> ChIP-seq
<input checked="" type="checkbox"/>	<input type="checkbox"/> Flow cytometry
<input checked="" type="checkbox"/>	<input type="checkbox"/> MRI-based neuroimaging

## Antibodies

Antibodies used

anti-H3 (Abcam, # ab1791; Lot #GR325252171-1; 1:2,000 working dilution)  
anti-H3K4me3 (Abcam, # ab8580; Lot # GR3275503-1; 1:1,000 working dilution)  
anti-H3K27ac (Abcam, # ab4729; Lot # GR3231988-1; 1:1,000 working dilution)  
anti-H3K27me3 (Millipore, # 07-449; Lot # 2919706; 1:1,000 working dilution)  
anti-ASH-2 (Abmart, # X3-G5EFZ3; Lot 31284-1; 1:1,000 working dilution)  
anti-β-tubulin (Santa Cruz, # sc-5274); Lot # B2218; 1:2,000-2,500 working dilution  
anti-ASH2L (Bethyl laboratories, # A300-489A; Lot # 2; 1:1,000 working dilution)  
anti-MLL1 (Bethyl laboratories, # A300-374A; Lot # 5; 1:500 working dilution)

Validation

All the antibodies used in this work are commercially available and have been published/cited.  
<https://www.citeab.com/antibodies/763778-ab1791-anti-histone-h3-antibody-nuclear-loading-con>  
<https://www.citeab.com/antibodies/763751-ab8580-anti-histone-h3-tri-methyl-k4-antibody-chi?des=E833EC8BF0454AA>  
<https://www.citeab.com/antibodies/778149-ab4729-anti-histone-h3-acetyl-k27-antibody-chip-g?des=EE13B14650FDA8F3>  
<https://www.citeab.com/antibodies/221356-07-449-anti-trimethyl-histone-h3-lys27-antibody?des=348CD7BFA0CC732E>  
<https://www.citeab.com/antibodies/835112-sc-5274-tubulin-antibody-d-10?des=517C27105F70CC7F>  
<https://www.citeab.com/antibodies/655121-a300-489a-ash2-antibody?des=32EFD81E08FF28C8>  
<https://www.citeab.com/antibodies/654913-a300-374a-ml1-antibody?des=620F371A0BC1D965>

The ASH-2 C. elegans antibody from Abmart (X3 -G5EFZ3) was tested against C. elegans treated with ash-2 RNAi and with purified recombinant C. elegans ASH-2.

## Eukaryotic cell lines

Policy information about [cell lines](#)

Cell line source(s)	HeLa EM-II cell line was a gift from JK Nandakumar (University of Michigan)
Authentication	STR
Mycoplasma contamination	HeLa EM-II cell line has been tested in the lab for mycoplasma contamination
Commonly misidentified lines (See <a href="#">ICLAC</a> register)	No commonly misidentified lines were used.

## Animals and other organisms

Policy information about [studies involving animals](#); [ARRIVE guidelines](#) recommended for reporting animal research

Laboratory animals	All C. elegans strains used in this study are detailed in Methods
Wild animals	The study did not involve wild animals
Field-collected samples	The study did not involve field-collected samples
Ethics oversight	No ethical approval or guidance is required.

Note that full information on the approval of the study protocol must also be provided in the manuscript.